Organometallics 1994, *13*, 1851-1864

Synthesis and Reactivity of Low-Valent Amido, Imido, Azavinylidene, and Nitrido Complexes of Tungsten

K. R. Powell, P. J. Pérez, L. Luan, S. G. Feng, P. S. White, M. Brookhart,* and J. L. Templeton*

Department of Chemistry, University of North Carolina, Chapel Hill, North Carolina 27599-3290

Received December 27, 1993[⊗]

Amido complexes Tp′(CO)$_2$W(NHR) [Tp′ = hydridotris(3,5-dimethylpyrazolyl)borate; R = Bu^t, **1a**; R = Ph, **1b**; R = Bu^n, **1c**; R = CH$_2$Ph, **1d**; R = H, **1e**] have been synthesized by reaction of the corresponding amine (NH$_2$R) with Tp′(CO)$_2$WI (**2**). These ambiphilic amido complexes have been utilized as precursors to both anionic imido complexes, Tp′(CO)$_2$W(NR)$^-$ (R = Ph, **3a**; R = CH$_2$Ph, **3b**; R = H, **3c**), and cationic imido complexes, Tp′(CO)$_2$W(NR)$^+$ (R = Bu^t, **5a**; R = Ph, **5b**; R = Bu^n, **5c**; R = CH$_2$Ph, **5d**; R = H, **6a**; R = CPh$_3$, **6b**). Treatment of the unstable anionic imido species **3a–c** with PhCH$_2$Br (**3a**) or MeI (**3b,c**) leads to the formation of dialkyl substituted amido complexes Tp′(CO)$_2$W(N(R)R′) (R = Ph, R′ = CH$_2$Ph, **4a**; R = CH$_2$Ph, R′ = Me, **4b**; R = R′ = Me, **4c**). The structures of **4a** and **4c** have been confirmed by X-ray diffraction. (**4a**·CH$_2$Cl$_2$ crystallizes in space group $P\bar{1}$ with $Z = 2$, $a = 11.452(2)$ Å, $b = 11.597(2)$ Å, $c = 14.144(2)$ Å, $\alpha = 86.78(1)°$, $\beta = 84.41(1)°$, $\gamma = 64.37(1)°$, $R = 3.7\%$, $R_w = 4.6\%$; **4c** crystallizes in space group $P\bar{1}$ with $Z = 2$, $a = 11.151(4)$ Å, $b = 11.702(3)$ Å, $c = 10.391(4)$ Å, $\alpha = 93.46(3)°$, $\beta = 108.56(3)°$, $\gamma = 63.20(3)°$, $R = 3.9\%$, $R_w = 4.3\%$.) Reactivity studies were carried out with the cationic nitrene complexes, Tp′(CO)$_2$W(NR)$^+$. Deprotonation of Tp′(CO)$_2$W(NCH$_2$R)$^+$ (R = Pr^n, **5c**; R = Ph, **5d**) yields azavinylidene complexes, Tp′(CO)$_2$W(N=CHR) (R = Pr^n, **7a**; R = Ph, **7b**). The barrier to rotation around the WNC unit of **7a** as determined by variable temperature NMR studies is 9.6 kcal/mol. Addition of LiBH$_4$ to the cationic nitrene complex **5b** results in formation of a formyl intermediate, Tp′(CO)(CHO)W(NPh) (**8**), which undergoes hydride migration from carbon to nitrogen to form the amido complex **1b** at −70 °C. Deprotonation of the parent nitrene cation Tp′(CO)$_2$W(NH)$^+$ (**6a**) or reaction of [(Ph$_3$P)$_2$N][N$_3$] with Tp′(CO)$_2$WI (**2**) yields an unstable nitrido complex Tp′(CO)$_2$WN (**9**). Complex **9** reacts with a variety of electrophiles (RX) to form both dicarbonyl, [Tp′(CO)$_2$W(NR)][X] (R = H, X = BF$_4^-$, **6a**; R = CPh$_3$, X = PF$_6^-$, **6b**; R = Me, X = OTf$^-$, **10**), as well as monocarbonyl, Tp′(CO)(X)W(NR) (R = Ts, X = Cl, **11a**; R = C(O)CH$_3$, X = Cl, **11b**; R = C(O)CH$_3$, X = OC(O)CH$_3$, **11c**), imido products. The X-ray structures of nitrene complexes Tp′(CO)$_2$W(NPh)$^+$ (**5b**) and Tp′(CO)ClW(NTs) (**11a**) reveal linear imido ligands for both cationic and neutral complexes with WN bond lengths of 1.775(7) and 1.78(1) Å, respectively. (**5b** crystallizes in space group $P2_1/n$ with $Z = 4$, $a = 10.301(2)$ Å, $b = 10.389(2)$ Å, $c = 27.816(7)$ Å, $\beta = 97.69(2)°$, $R = 3.6\%$, $R_w = 4.5\%$; **11a** crystallizes in space group $P2_1$ with $Z = 2$, $a = 8.222(3)$ Å, $b = 17.256(6)$ Å, $c = 9.561(4)$ Å, $\beta = 100.85(3)°$, $R = 4.0\%$, $R_w = 4.6\%$.)

Introduction

Despite the plethora of structurally characterized transition metal nitrene (or imido) complexes,[1,2] the reactivity of the ligand itself has received relatively little attention. Although nitrene intermediates have been proposed in the Haber ammonia synthesis,[3] nitrile reduction,[4] and ammoxidation of propylene,[5] the majority of isolated nitrene complexes contain linear, unreactive imido ligands, a property compatible with their role as ligands for the stabilization of high metal oxidation states.[2] Complexes with bent imido ligands have been structurally characterized as well. In general, bending of an imido ligand occurs when lone pair donation would result in a complex with an electron count exceeding eighteen.[6] These linear and bent bonding modes suggest structural analogies with oxo, carbene, and carbyne ligands.[2b] If this analogy between nitrene and oxo or carbene systems is extended to reactivity, imido complexes have potential as nitrene transfer agents in organic synthesis. One of the first examples of this utility was the amination of olefins with osmium imido reagents developed by Sharpless and coworkers.[7]

In terms of reactivity, the nitrene ligand may be nucleophilic or electrophilic at nitrogen. Many nucleophilic imido species react with aldehydes or ketones to give organic imines.[8] For example, the putative zerovalent complex (CO)$_5$W(NPh) reacts with a variety of electrophilic aldehydes, ketones, and thioketones to produce free

---

[⊗] Abstract published in *Advance ACS Abstracts*, April 1, 1994.

(1) According to IUPAC rules, the term "imido" is preferred to "nitrene" to describe M(NR) complexes. "Nitrene" is a familiar term which has found widespread acceptance and has been used more frequently, but not exclusively, to describe species which contain an electron deficient nitrogen. Herein, we use both the terms "imido" and "nitrene" to describe M(NR) complexes.

(2) For reviews of imido complexes, see: (a) Nugent, W. A.; Haymore, B. L. *Coord. Chem. Rev.* **1980**, *31*, 123. (b) Nugent, W. A.; Mayer, J. M. *Metal-Ligand Multiple Bonds*; Wiley-Interscience: New York, 1988. (c) Cenini, S.; La Monica, G. *Inorg. Chim. Acta* **1976**, *18*, 279.

(3) Fjare, D. E.; Gladfelter, W. L. *J. Am. Chem. Soc.* **1981**, *103*, 1572.

(4) Andrews, M. A.; Kaesz, H. D. *J. Am. Chem. Soc.* **1979**, *101*, 7255.

(5) Burrington, J. D.; Grasselli, R. K. *J. Catal.* **1979**, *59*, 79.

(6) Et$_2$dtc = *N,N*′-diethyldithiocarbamate. (a) Maatta, E. A.; Haymore, B. L.; Wentworth, R. A. D. *Inorg. Chem.* **1980**, *19*, 1055. (b) Maatta, E. A.; Haymore, B. L.; Wentworth, R. A. D. *Inorg. Chem.* **1979**, *18*, 2409.

(7) (a) Sharpless, K. B.; Teranishi, A. Y.; Bäckvall, J.-E. *J. Am. Chem. Soc.* **1977**, *99*, 3120. (b) Chong, A. O.; Oshima, K.; Sharpless, K. B. *J. Am. Chem. Soc.* **1977**, *99*, 3420. (c) Patrick, D. W.; Truesdale, L. K.; Biller, S. A.; Sharpless, K. B. *J. Org. Chem.* **1978**, *43*, 2628.

0276-7333/94/2313-1851$04.50/0

organic imines.[9] Bending of the imido ligand is generally believed to increase its nucleophilicity. The classic example of this behavior is the protonation (or methylation) of a single imido ligand of $(Et_2dtc)_2Mo(NPh)_2$ which contains one linear and one bent imido unit.[6] More recently, a reactive low valent linear nitrene complex, Cp^*IrNBu^t, has been reported which reacts with MeI, CO, and $CNBu^t$ and also undergoes 2 + 2 reactions with CO_2 and an alkyne.[10] Bergman and Wolczanski have proposed that transient nucleophilic zirconium imido species, $[Cp_2Zr{=}NBu^t]$ and $[(Bu^t{}_3SiNH)_2Zr{=}NSiBu^t{}_3]$, respectively, promote intermolecular C—H bond activation.[11] Likewise, deuteration of the amido protons of $(Bu^t{}_3SiNH)_2(Et_2O)Ti{=}NSiBu^t{}_3$ in the presence of C_6D_6 is proposed to occur via the transient imido species $[(Bu^t{}_3SiNH)_2Ti{=}NSiBu^t{}_3]$.[12]

Nitrene complexes with reactivity patterns that indicate electrophilic character at nitrogen are rare. Electrophilic nitrenes tend to be difficult to observe or isolate, and details of their reactivity are not well understood. The aforementioned amination of olefins by osmium imido complexes has been proposed to proceed by initial association of the olefin with an electron deficient nitrene ligand.[7] Another early example of apparent electrophilicity at nitrogen is the reaction of $(Me_3SiO)_2Cr(NBu^t)_2$ with Ph_2Zn which yields *tert*-butylaniline upon hydrolysis.[13] Sulfuric or hydrochloric acid decomposition of $[Ir(NH_3)_5N_3]^{2+}$ to give $[Ir(NH_3)_5NH_2OSO_3]^{2+}$ or $[Ir(NH_3)_5NH_2Cl]^{3+}$, respectively, is proposed to proceed through an electrophilic nitrene intermediate $[Ir(NH_3)_5NH]^{3+}$ which reacts with HSO_4^- or Cl^-, respectively.[14] A number of electrophilic nitrene complexes add phosphine at nitrogen to form phosphine imides. Ambiphilic $(CO)_5W(NPh)$, noted earlier for its nucleophilic reactivity, is trapped with PPh_3 to form the coordinated phosphine imide.[15] The related heteroatom stabilized nitrene $(CO)_5W(NNMe_2)$ undergoes CO substitution with PPh_3 and DPPE in preference to phosphine addition at nitrogen although reaction with DPPM yields the metallacyclic phosphinimine, $(CO)_4\overline{W(PPh_2CH_2PPh_2)N}NMe_2$.[16] Likewise, the putative nitrene intermediate from the reaction of *fac*-$Mo(CO)_3(NCCH_3)_2PPh_3$ with 8-azidoquinoline is trapped by phosphine to yield $(CO)_4\overline{Mo[N(PPh_3)(C_9H_6N})]$.[17] Ruthenium and chromium porphyrin imido complexes react with PPh_3 to yield the free phosphine imides, $Ph_3P{=}NR$.[18] Similarly, the homoleptic imido complex $Os(N\text{-}2,6\text{-}C_6H_3Pr^i{}_2)_3$ reacts with PMe_2Ph to yield $PhMe_2P{=}NAr$ and $Os(NAr)_2(PMe_2Ph)_2$.[19] Additionally, $Mo(NTs)_2(Et_2dtc)_2$ carries out similar nitrene transfer to phosphine catalytically using PhMeSNTs or Ph_3SbNTs as the nitrene source.[20]

Recent reports of enantioselective nitrene transfer in catalytic aziridination reactions[21] are particularly significant because of promising applications to asymmetric synthesis.[22] Jacobsen and co-workers have developed chiral diimine–copper(I) complexes which effect enantioselective aziridination of a variety of olefins utilizing $PhI{=}NTs$ as the nitrene source.[21a] Concurrently, Evans has reported good yields of aziridines generated by enantioselective nitrene transfer from $PhI{=}NTs$ to olefins catalyzed by chiral bis(oxazoline)copper complexes.[21b] Previously, a number of copper systems that catalyze nitrene transfer from $PhI{=}NTs$ to olefins were known[21c,d,23] although only two enantioselective reactions had ever been described (both with chiral bis(oxazoline) ligands).[21c,d] The intermediacy of electrophilic metal nitrenes has been proposed in these copper systems[21,23] as well as in earlier reports of manganese and iron porphyrin catalyzed nitrene transfer systems.[24] In catalytic cyclopropanation reactions a catalytic carbene species has only recently been observed;[25] the putative nitrene intermediate is elusive as well.

This paper reports general routes to cationic, anionic, and neutral tungsten nitrene complexes; portions have been communicated earlier.[26] Neutral amido complexes, $Tp'(CO)_2W(NHR)$ [R = Bu^t (**1a**), Ph (**1b**), Bu^n (**1c**), CH_2Ph (**1d**), and H (**1e**)], serve as precursors to both cationic, $Tp'(CO)_2W(NR)^+$, and anionic, $Tp'(CO)_2W(NR)^-$, imido complexes. The nature of the nitrene nitrogen of the cationic complexes appears to be electrophilic while that of the anionic complexes is nucleophilic. The conversion of cationic nitrene complexes to amido, azavinylidene, and nitrido complexes is described in detail. The synthetic utility of the nitrido complex, $Tp'(CO)_2WN$, as a precursor to new imido complexes is established.

---

(8) (a) Cotton, F. A.; Hall, W. T. *J. Am. Chem. Soc.* **1979**, *101*, 5094. (b) Rocklage, S. M.; Schrock, R. R. *J. Am. Chem. Soc.* **1980**, *102*, 7808. (c) Rocklage, S. M.; Schrock, R. R. *J. Am. Chem. Soc.* **1982**, *104*, 3077. (d) Nugent, W. A. *Inorg. Chem.* **1983**, *22*, 965.

(9) Arndtsen, B. A.; Sleiman, H. F.; Chang, A. K.; McElwee-White, L. *J. Am. Chem. Soc.* **1991**, *113*, 4871.

(10) (a) Glueck, D. S.; Hollander, F. J.; Bergman, R. G. *J. Am. Chem. Soc.* **1989**, *111*, 2719. (b) Glueck, D. S.; Wu, J.; Hollander, F. J.; Bergman, R. G. *J. Am. Chem. Soc.* **1991**, *113*, 2041.

(11) (a) Cummins, C. C.; Baxter, S. M.; Wolczanski, P. T. *J. Am. Chem. Soc.* **1988**, *110*, 8731. (b) Walsh, P. J.; Hollander, F. J.; Bergman, R. G. *J. Am. Chem. Soc.* **1988**, *110*, 8729. (c) Walsh, P. J.; Baranger, A. M.; Bergman, R. G. *J. Am. Chem. Soc.* **1992**, *114*, 1708.

(12) Cummins, C. C.; Schaller, C. P.; Van Duyne, G. D.; Wolczanski, P. T. *J. Am. Chem. Soc.* **1991**, *113*, 2985.

(13) Nugent, W. A.; Harlow, R. L. *J. Am. Chem. Soc.* **1980**, *102*, 1759.

(14) (a) Lane, B. C.; McDonald, J. W.; Basolo, F.; Pearson, R. G. *J. Am. Chem. Soc.* **1972**, *94*, 3786. (b) Gafney, H. D.; Reed, J. L.; Basolo, F. *J. Am. Chem. Soc.* **1973**, *95*, 7998.

(15) Sleiman, H. F.; Mercer, S.; McElwee-White, L. *J. Am. Chem. Soc.* **1989**, *111*, 8007.

(16) Arndtsen, B. A.; Sleiman, H. F.; McElwee-White, L.; Rheingold, A. L. *Organometallics* **1993**, *12*, 2440.

(17) Fourquet, J. L.; Leblanc, M.; Saravanamuthu, A.; Bruce, M. R. M.; Bruce, A. E. *Inorg. Chem.* **1991**, *30*, 3241.

(18) (a) Huang, J.-S.; Che, C.-M.; Poon, C.-K. *J. Chem. Soc., Chem. Commun.* **1992**, 161. (b) Elliot, R. L.; Nichols, P. J.; West, B. O. *Polyhedron* **1987**, *6*, 2191.

(19) Anhaus, J. T.; Kee, T. P.; Schofield, M. H.; Schrock, R. R. *J. Am. Chem. Soc.* **1990**, *112*, 1642.

(20) Et_2dtc = *N,N'*-diethyldithiocarbamate. Harlan, E. W.; Holm, R. H. *J. Am. Chem. Soc.* **1990**, *112*, 186.

(21) (a) Li, Z.; Conser, K. R.; Jacobsen, E. N. *J. Am. Chem. Soc.* **1993**, *115*, 5326. (b) Evans, D. A.; Faul, M. M.; Bilodeau, M. T.; Anderson, B. A.; Barnes, D. M. *J. Am. Chem. Soc.* **1993**, *115*, 5328. (c) Evans, D. A.; Faul, M. M.; Bilodeau, M. T. *J. Org. Chem.* **1991**, *56*, 6744. (d) Lowenthal, R. E.; Masamune, S. *Tetrahedron Lett.* **1991**, *32*, 7373.

(22) (a) Swift, G.; Swern, D. *J. Org. Chem.* **1967**, *32*, 511. (b) Tseng, C. C.; Terashima, S.; Yamada, S.-i. *Chem. Pharm. Bull.* **1977**, *25*, 166. (c) Padwa, A.; Woolhouse, A. D. Aziridines, Azirines, and Fused-ring Derivatives. In *Comprehensive Heterocyclic Chemistry*; Lwowski, W., Ed.; Pergamon Press: Oxford, U.K., 1984; Vol. 7.

(23) (a) Evans, D. A.; Woerpel, K. A.; Hinman, M. M.; Faul, M. M. *J. Am. Chem. Soc.* **1991**, *113*, 726. (b) O'Connor, K. J.; Wey, S.-J.; Burrows, C. J. *Tetrahedron Lett.* **1992**, *33*, 1001. (c) Pérez, P. J.; Brookhart, M.; Templeton, J. L. *Organometallics* **1993**, *12*, 261.

(24) (a) Mansuy, D.; Mahy, J.-P.; Dureault, A.; Bedi, G.; Battioni, P. *J. Chem. Soc., Chem. Commun.* **1984**, 1161. (b) Mansuy, D.; Mahy, J.-P.; Bedi, G.; Battioni, P. *J. Chem. Soc., Perkin Trans. 2* **1988**, 1517. (c) Groves, J. T.; Takahashi, T. *J. Am. Chem. Soc.* **1983**, *105*, 2073.

(25) Smith, D. A.; Reynolds, D. N.; Woo, L. K. *J. Am. Chem. Soc.* **1993**, *115*, 2511.

(26) (a) Luan, L.; White, P. S.; Brookhart, M.; Templeton, J. L. *J. Am. Chem. Soc.* **1990**, *112*, 8190. (b) Luan, L.; Brookhart, M.; Templeton, J. L. *Organometallics* **1992**, *11*, 1433. (c) Pérez, P. J.; Luan, L.; White, P. S.; Brookhart, M.; Templeton, J. L. *J. Am. Chem. Soc.* **1992**, *114*, 7928.

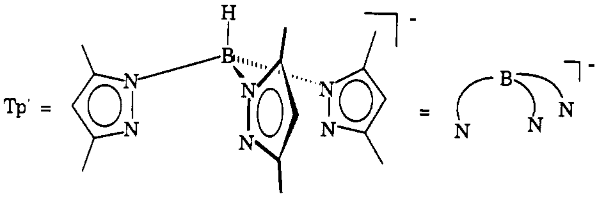

Figure 1. Hydridotris(3,5-dimethylpyrazolyl)borate.

Results and Discussion

Synthesis and Reactivity of Tp′(CO)$_2$W(N(R)R′). Reaction of Tp′(CO)$_3$WI [Tp′ = hydridotris(3,5-dimethylpyrazolyl)borate (Figure 1)] with excess amine (NH$_2$Bu^t or NH$_2$Ph) in refluxing THF leads to the formation of amido(dicarbonyl)tungsten(II) d^4 complexes Tp′(CO)$_2$W(NHR) [R = Bu^t (**1a**) and Ph (**1b**)] (eq 1). We believe that this reaction proceeds through an unsaturated dicarbonyl iodide species that is observed by IR spectroscopy (1944, 1844 cm^{-1}) during the course of the reaction. These stretching frequencies are identical to those observed when Tp′(CO)$_3$WI is refluxed in THF in the absence of amine to form a paramagnetic 16 electron species, Tp′(CO)$_2$WI (**2**) (eq 2), which can be isolated as an orange microcrystalline solid.

$$\mathrm{Tp'(CO)_3WI} \xrightarrow[\substack{-\mathrm{CO} \\ \mathrm{THF,\ reflux}}]{\mathrm{NH_2R}} \mathrm{Tp'(CO)_2W}\overset{\leftarrow}{=}\mathrm{NHR} + [\mathrm{NH_3R}]\mathrm{I} \qquad (1)$$

R = Bu^t (**1a**), Ph (**1b**)

$$\mathrm{Tp'(CO)_3WI} \xrightarrow[\mathrm{THF,\ reflux}]{-\mathrm{CO}} \underset{\mathbf{2}}{\mathrm{Tp'(CO)_2WI}} \qquad (2)$$

Tp′(CO)$_2$WI (**2**) reacts with amines under relatively mild conditions and, for this reason, is more satisfactory than Tp′(CO)$_3$WI for the synthesis of Tp′(CO)$_2$W(NHR) (**1a**–**e**) products (eq 3). These complexes (**1a**–**e**) have been isolated as solids after chromatography or crystallization. They are stable for long periods of time when stored under nitrogen, except for the NH$_2$ derivative (**1e**) which decomposes after 1 or 2 weeks even at −20 °C.

$$\underset{\mathbf{2}}{\mathrm{Tp'(CO)_2WI}} \xrightarrow{\mathrm{NH_2R}} \mathrm{Tp'(CO)_2W}\overset{\leftarrow}{=}\mathrm{NHR} + [\mathrm{NH_3R}]\mathrm{I} \qquad (3)$$

complex	R	conditions
1a	Bu^t	CH$_2$Cl$_2$, 25 °C
1b	Ph	CH$_2$Cl$_2$, 25 °C
1c	Bu^n	THF, 25 °C
1d	CH$_2$Ph	CH$_2$Cl$_2$, 25 °C
1e	H	CH$_2$Cl$_2$, −50 °C

Spectroscopic studies of **1a**–**e** support the formulation of these products as neutral amido complexes with C_s symmetry. Carbonyl stretching frequencies near 1910 and 1790 cm^{-1} (Table 1) for **1a**–**e** are compatible with expectations for neutral d^4 complexes.[27] The presence of a molecular mirror plane is evident from both the 2:1 pattern for the pyrazole rings in the ^{1}H and ^{13}C NMR spectra and the single ^{13}C resonance for the two carbonyl ligands. C_s symmetry on the NMR time scale is compatible with either a static NHR fragment that lies in the mirror plane or with rapid rotation around the W–N bond. If the amido ligand is static and lies in the mirror plane, there are two possible isomers (see Figure 2), one with R oriented away from the bulky Tp′ ligand (anti) and one with R located near the Tp′ ligand (syn).

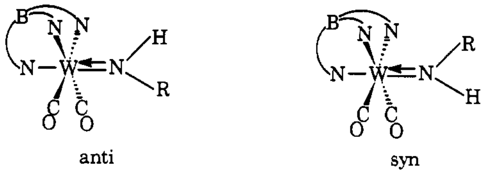

Figure 2. Anti and syn isomers of Tp′(CO)$_2$W(NHR).

^{1}H NMR signals in the range 10–16 ppm are diagnostic for coordinated amido protons (N*H*R). Tp′(CO)$_2$W(NHBu^n) (**1c**) and Tp′(CO)$_2$W(NHCH$_2$Ph) (**1d**) exist as a 6:1 mixtures of two isomers in solution at room temperature, as indicated by their ^{1}H NMR signals for the amido hydrogens at 13.7 and 11.9 ppm (**1c**) and 13.6 and 11.8 ppm (**1d**), respectively (see Table 2 for ^{1}H NMR data). Tp′(CO)$_2$W(NHPh) (**1b**) also exists as a mixture of two isomers in solution. In this case, the major isomer can be separated by crystallization and obtained as a solid. Kinetics experiments on formation of the second isomer of **1b** have been carried out at 22 °C. Upon dissolution of crystals of the major isomer of **1b** (15.3 ppm, N*H*) in CD$_2$Cl$_2$, the minor isomer (13.0 ppm, N*H*) is observed to grow in over 5 days. The minor isomer accounts for 11.8% of the total material at equilibrium which corresponds to $K_{eq} = 0.13$. The interconversion of the two isomers (eq 4) is a first order process with rates of interconversion $k_1 = 7.0 \times 10^{-6}$ s^{-1} and $k_{-1} = 5.2 \times 10^{-5}$ s^{-1} corresponding to $\Delta G^{\ddagger} = 24.2$ kcal/mol and $\Delta G^{\ddagger} = 23.0$ kcal/mol, respectively.

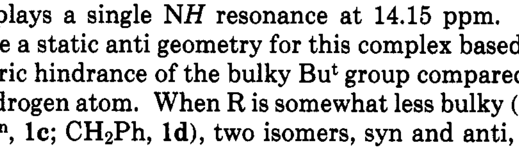

(4)

For the Tp′(CO)$_2$W(NHR) complexes we propose that restricted rotation around the tungsten amide multiple bond is the mode of isomerization. When R is very bulky (Bu^t, **1a**), only the favored isomer is observed. Complex **1a** displays a single N*H* resonance at 14.15 ppm. We propose a static anti geometry for this complex based on the steric hindrance of the bulky Bu^t group compared to the hydrogen atom. When R is somewhat less bulky (Ph, **1b**; Bu^n, **1c**; CH$_2$Ph, **1d**), two isomers, syn and anti, are observed in solution.

Two broad signals at 13.5 and 11.6 ppm in the room temperature ^{1}H NMR spectrum of the parent amido complex Tp′(CO)$_2$W(NH$_2$) (**1e**) are assigned to the two amido protons. These signals coalesce at 103 °C, corresponding to $\Delta G^{\ddagger} = 17$ kcal/mol. Thus this barrier to rotation is significantly lower than the barriers for interconversion of the syn and anti isomers of Tp′(CO)$_2$W(NHPh) (**1b**) described above. Rotation around the tungsten–nitrogen bond in Tp′(CO)$_2$W(NHPh) (**1b**) may be expected to be more restricted than that in Tp′(CO)$_2$W(NH$_2$) (**1e**) based on the steric encumbrance of the phenyl group which must rotate past the Tp′ methyl groups.

Deprotonation of Tp′(CO)$_2$W(NHR) amido complexes **1b**, **1d**, and **1e** with LDA (lithium diisopropylamide) (**1d** and **1e**) or Bu^{t}Li (**1b**) yields reactive dicarbonyl species. On the basis of the low carbonyl stretching frequencies (1750 and 1652 cm^{-1}, **1b**; 1858 and 1720 cm^{-1}, **1d**; 1861 and 1724 cm^{-1}, **1e**), we propose that anionic tungsten nitrene

---

[27] Feng, S. G.; Templeton, J. L. *Organometallics* **1992**, *11*, 2168.

Table 1. IR Data[a] for 1a–e, 2, 4a–c, 5a–d, 6a,b, 7a,b, 9, 10, and 11a–c

complex	ν(CO)[b]	other	ν(BH)[c]	ν(PF)[c]
1a, $Tp'(CO)_2W(NHBu^t)$	1910, 1782	3260, 3121 (N—H)[c]	2546	
1b, $Tp'(CO)_2W(NHPh)$	1900, 1786	3231, 3138 (N—H)[c]	2548	
1c, $Tp'(CO)_2W(NHBu^n)$	1911, 1794	3260, 3125 (N—H)[c]	2540	
1d, $Tp'(CO)_2W(NHCH_2Ph)$	1910, 1784	3311, 3261 (N—H)[c]	2544	
1e, $Tp'(CO)_2W(NH_2)$	1915, 1793	3395, 3305 (N—H)[c]	2540	
2, $Tp'(CO)_2WI$	1944, 1844			
3a, $[Li][Tp'(CO)_2W(NPh)]$	1750, 1652			
3b, $[Li][Tp'(CO)_2W(NCH_2Ph)]$	1858, 1720			
3c, $[Li][Tp'(CO)_2W(NH)]$	1861, 1724			
4a, $Tp'(CO)_2W(N(Ph)CH_2Ph)$	1914, 1787			
4b, $Tp'(CO)_2W(N(Me)CH_2Ph)$	1904, 1777		2540	
4c, $Tp'(CO)_2W(NMe_2)$	1904, 1777		2536	
5a, $[Tp'(CO)_2W(NBu^t)][PF_6]$	2081, 2003			
5b, $[Tp'(CO)_2W(NPh)][PF_6]$	2079, 2006		2589	849
5c, $[Tp'(CO)_2W(NBu^n)][PF_6]$	2082, 2004		2577	841
5d, $[Tp'(CO)_2W(NCH_2Ph)][PF_6]$	2083, 2006		2565	843
6a, $[Tp'(CO)_2W(NH)][PF_6]$	2092, 2017	3328 (N—H)[c]	2577	844
6b, $[Tp'(CO)_2W(NCPh_3)][PF_6]$	2083, 2008		2582	841
7a, $Tp'(CO)_2W(N{=}CHPr^n)$	1923, 1815	1628 (C=N)[b]	2575	
7b, $Tp'(CO)_2W(N{=}CHPh)$	1942, 1830	1559 (C=N)[b]	2582	
9, $Tp'(CO)_2WN$	2041, 1944			
10, $[Tp'(CO)_2W(NMe)][PF_6]$	2083, 2006		2581	844
11a, $Tp'(CO)ClW(NTs)$	1969		2557	
11b, $Tp'(CO)ClW(NC(O)CH_3)$	1954	1674 (-C(O)-)[b]	2559	
11c, $Tp'(CO)(OC(O)CH_3)W(NC(O)CH_3)$	1948	1674, 1645 (-C(O)-)[b]		

[a] In cm^{-1}. [b] CH_2Cl_2 solution. [c] Nujol mull.

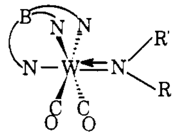

Figure 3. Schematic representation of amido orientation.

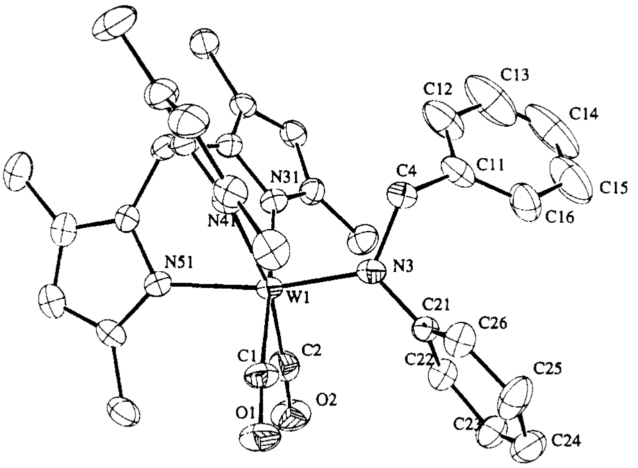

Figure 4. ORTEP diagram of $Tp'(CO)_2W(N(Ph)CH_2Ph)$ (**4a**).

complexes, $[Li][Tp'(CO)_2W(NR)]$ (**3a–c**), are formed (eq 5). These anionic dicarbonyl nitrene complexes are sus-

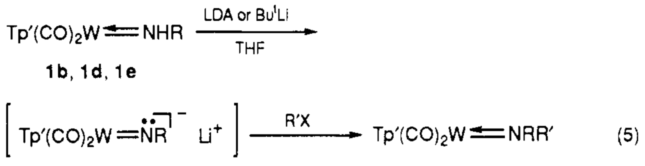

(5)

complex	R	complex	R	R'X
3a	Ph	**4a**	Ph	$PhCH_2Br$
3b	CH_2Ph	**4b**	CH_2Ph	MeI
3c	H			

ceptible to protonation by traces of moisture to reform the starting material, $Tp'(CO)_2W(NHR)$. When quenched with alkylating agents at low temperature, however, dialkyl substituted amido complexes **4a–c** are formed. In the reaction of $Tp'(CO)_2W(NH_2)$ (**1e**) with base followed by MeI (eq 6), double alkylation occurs. Under these reaction

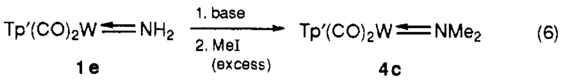

(6)

conditions, perhaps any $Tp'(CO)_2W(NHMe)$ formed is susceptible to deprotonation which is followed by methylation by excess MeI.

Spectroscopic data for **4a–c** are similar to those observed for **1a–e** (vide supra; see Tables 1 and 2). Consequently, we propose a similar structural formulation for **4a–c** (Figure 3). Single crystal X-ray diffraction studies of $Tp'(CO)_2W(N(Ph)CH_2Ph)$ (**4a**) and $Tp'(CO)_2W(NMe_2)$ (**4c**) unequivocally establish the geometry of these complexes and confirm that the NRR' moiety lies in the molecular mirror plane. Figures 4 and 5 show ORTEP diagrams of $Tp'(CO)_2W(N(Ph)CH_2Ph)$ (**4a**) and $Tp'(CO)_2W(NMe_2)$ (**4c**). The crystallographic data and collection parameters for **4a** and **4c** are given in Table 3; Tables 4–7 present atomic parameters and selected bond distances and angles for **4a** and **4c**. The 1.981(6)-Å (**4a**) and 1.956(5)-Å (**4c**) W–N distances are appropriate for tungsten–nitrogen double bonds, as found in Chisholm's tungsten amido complexes.[28] Although tungsten hydrazido species are sometimes considered to have metal–nitrogen double bonds, the two-coordinate nitrogen in $W–N–NR_2$ systems exhibits W–N distances well below 2.0 Å and more in the range typical of tungsten nitrenes.[2b] The amide nitrogens are roughly sp^2 hybridized on the basis of bond angles: W(1)–N(3)–C(4), 122.7(4)°; W(1)–N(3)–C(21), 125.6(4)°; and C(4)–N(3)–C(5), 111.1(5)° (**4a**) and W(1)–N(3)–C(4), 128.7(5)°; W(1)–N(3)–C(5), 121.2(4)°; and C(4)–N(3)–C(5), 110.1(6)° (**4c**). The WNRR' skeletons are planar and are located in the mirror plane of the molecules. The phenyl

---

[28] Buhro, W. E.; Chisholm, M. H.; Folting, K.; Huffman, J. C.; Martin, J. D.; Streib, W. E. *J. Am. Chem. Soc.* **1992**, *114*, 557.

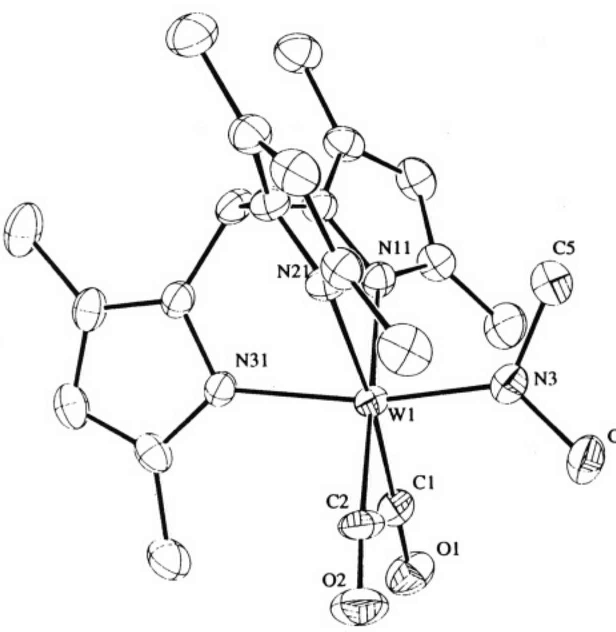

Figure 5. ORTEP diagram of $Tp'(CO)_2W(NMe_2)$ (**4c**).

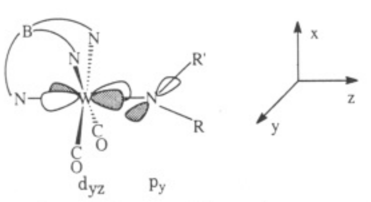

Figure 6. Drawing of the metal dπ–nitrogen pπ interactions for $Tp'(CO)_2W(NRR')$.

group of **4a** is situated anti to the Tp′ ligand, as expected on the basis of the relative sizes of the phenyl and benzyl groups.

As shown in Figure 6 and explained below, for acute OC–M–CO angles optimal π-bonding occurs when the amide (NRR′) is in the mirror plane.[29] This vertical arrangement allows donation from the nitrogen (p_y) into the lone vacant dπ orbital (d_{yz}). The two filled dπ orbitals (d_{xz} and $d_{x^2-y^2}$) are stabilized by back-bonding to the two π-acid carbonyl ligands. Preferential stabilization of the filled d_{xz} orbital occurs when the angle between the carbonyls is decreased to less than 90° in order to increase the overlap of the CO π* orbitals with the filled d_{xz} orbital while overlap with the vacant d_{yz} orbital decreases. Intensity measurements for the carbonyl infrared stretches of this series of $Tp'(CO)_2W(N(R)R')$ complexes indicate that the acute angle between the carbonyls is maintained in solution (80°, **1b**; 86°, **1d**; 85°, **4b**); by X-ray diffraction the angles between the carbonyls of **4a** and **4c** are observed to be 74.6(3) and 71.8(3)°, respectively, in the solid state.

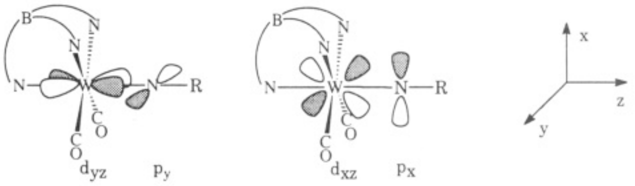

Figure 7. Drawings of the metal dπ–nitrogen pπ interactions for $Tp'(CO)_2W(NR)^+$ (**5a–d**, **6a,b**, **10**) and $Tp'(CO)_2WN$ (**9**).

Synthesis and Reactivity of $[Tp'(CO)_2W(NR)][PF_6]$. $Tp'(CO)_2W(NHR)$ complexes exhibit ambiphilic behavior at nitrogen and can act as either proton or hydride donors to form nitrene complexes. As discussed earlier, anionic nitrene complexes are formed when $Tp'(CO)_2W(NHR)$ [R = Ph (**1b**), R = CH_2Ph (**1d**), and R = H (**1e**)] compounds are treated with strong bases. Remarkably, the amido hydrogen can also be removed as a hydride. Treatment of $Tp'(CO)_2W(NHR)$ [R = Bu^t (**1a**), R = Ph (**1b**), R = Bu^n (**1c**), and R = CH_2Ph (**1d**)] with $[Ph_3C][PF_6]$ at low temperature yields cationic dicarbonylimidotungsten(IV) d^2 complexes, $[Tp'(CO)_2W(NR)][PF_6]$ [(R = Bu^t (**5a**), R = Ph (**5b**), R = Bu^n (**5c**), and R = CH_2Ph (**5d**), respectively] (eq 7). Similar treatment of $Tp'(CO)_2W(NH_2)$ (**1e**) with $[Ph_3C][PF_6]$ yields not only the expected hydride abstraction product, $[Tp'(CO)_2W(NH)][PF_6]$ (**6a**), but also another cationic nitrene complex, $[Tp'(CO)_2W(NCPh_3)][PF_6]$ (**6b**) (eq 8). Complexes **6a** and **6b**, present in a 4:1 ratio, respectively, are separable by crystallization.

$$\underset{\mathbf{1a,\ 1b,\ 1c,\ 1d}}{\mathrm{Tp'(CO)_2W{\Leftarrow}NHR}} \xrightarrow[\mathrm{CH_2Cl_2,\ 0\ ^\circ C}]{[\mathrm{Ph_3C}][\mathrm{PF_6}]} \underset{\mathbf{5a,\ 5b,\ 5c,\ 5d}}{\left[\mathrm{Tp'(CO)_2W{\equiv}NR}\right]^+} \qquad (7)$$

R = Bu^t (**a**), Ph (**b**), Bu^n (**c**), CH_2Ph (**d**)

$$\underset{\mathbf{1e}}{\mathrm{Tp'(CO)_2W{\Leftarrow}NH_2}} \xrightarrow[\mathrm{CH_2Cl_2,\ -30\ ^\circ C}]{[\mathrm{Ph_3C}][\mathrm{PF_6}]} \underset{\mathbf{6a}}{\left[\mathrm{Tp'(CO)_2W{\equiv}NH}\right]^+} + \underset{\mathbf{6b}}{\left[\mathrm{Tp'(CO)_2W{\equiv}NCPh_3}\right]^+} \qquad (8)$$

Complexes **5a–d** and **6a,b** are obtained as crystalline solids upon crystallization from $CH_2Cl_2{:}Et_2O$ and are stable when stored under nitrogen. The stability of these cationic dicarbonyl nitrene complexes is noteworthy because they contain both π-acceptor and π-donor ligands. The origin of this stability lies in the d^2 configuration.[2b] The single filled dπ orbital ($d_{x^2-y^2}$) can back-bond to both carbonyl ligands while the two empty dπ orbitals (d_{xz} and d_{yz}) are free to interact with the two filled nitrogen p orbitals of the NR^{2-} moiety (Figure 7) thereby fulfilling the electronic demands of both types of ligands. The high infrared carbonyl stretching frequencies for **5a–d** and **6a,b** (Table 1) are characteristic of an electron deficient metal center. Large two bond tungsten to carbon coupling in the nitrene ligand (26–31 Hz; Table 2) suggests sp hybridization at nitrogen.[30] The linear NR unit can be labeled as a nitrene and considered as a four electron donor in the neutral counting formalism, or it can be counted as a six electron donor imido dianion. Ultimately, the choice of which formalism to apply here is a matter of preference. X-ray diffraction studies of $[Tp'(CO)_2W(NPh)][PF_6]$ (**5b**) confirm that the WNC linkage is indeed nearly linear (171.6(6)°) (see Figure 8 for an ORTEP diagram, Table 3 for crystallographic data collection parameters, Table 8 for atomic parameters, and Table 9 for selected bond distances and angles). The W–N bond distance is short (1.755(7) Å), consistent with multiple bonding. The angle between the two carbonyl ligands is 93.7(4)°, which allows for optimal π-bonding of the CO π* orbitals with the single, filled dπ metal orbital ($d_{x^2-y^2}$).

---

(29) (a) Templeton, J. L.; Ward, B. C. *J. Am. Chem. Soc.* **1980**, *102*, 6568. (b) Kubacek, P.; Hoffmann, R. *J. Am. Chem. Soc.* **1981**, *103*, 4320. (c) Templeton, J. L.; Winston, P. B.; Ward, B. C. *J. Am. Chem. Soc.* **1981**, *103*, 7713.

(30) Feng, S. G.; Luan, L.; White, P. S.; Brookhart, M.; Templeton, J. L.; Young, C. *Inorg. Chem.* **1991**, *30*, 2582.

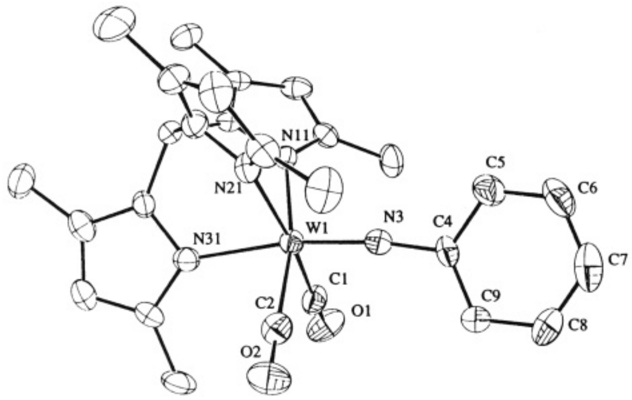

Figure 8. ORTEP diagram of $[Tp'(CO)_2W(NPh)][PF_6]$ (**5b**).

Cationic complexes which have a methylene unit adjacent to nitrogen, $[Tp'(CO)_2W(NCH_2R)][PF_6]$ (R = Pr^n (**5c**) and R = Ph (**5d**)), are readily deprotonated at the β-carbon with Et_3N to form azavinylidene complexes, $Tp'(CO)_2W(N{=}CHR)$ [R = Pr^n (**7a**) and R = Ph (**7b**), respectively] (eq 9).[31] The acidity of the hydrogen on the carbon α to nitrogen is attributed to the electron-accepting role played by the nitrene nitrogen.[32] Formation of a neutral product is evident by monitoring the carbonyl stretching frequencies. These frequencies (1923, 1815 cm^{-1} (**7a**) and 1942, 1830 cm^{-1} (**7b**)) are somewhat higher than those observed for the $Tp'(CO)_2W(N(R)R')$ complexes (**1a–e** and **4a–c**) (see Table 1) which is consistent with net oxidative removal of dihydrogen which formally relates the $NHCH_2R$ and $N{=}CHR$ ligands. The $\nu_{N=C}$ frequencies (1628 cm^{-1} (**7a**) and 1559 cm^{-1} (**7b**)) are typical for azavinylidene complexes.[33] Large two-bond tungsten to carbon coupling (27 Hz (**7a**) and 26 Hz (**7b**)), as in the cationic nitrene complexes, is indicative of a linear WNC linkage.[30] Protonation of the azavinylidene complexes (**7a** and **7b**) with HBF_4 re-forms the corresponding cationic nitrene complexes $Tp'(CO)_2W(NCH_2R)^+$ (eq 9).

$$\left[\mathrm{Tp'(CO)_2W{\equiv}NCH_2R}\right]^{+} \underset{H^{+}}{\overset{Et_3N}{\rightleftharpoons}} \mathrm{Tp'(CO)_2W{=}N{=}CHR} \qquad (9)$$

5c, **5d** **7a**, **7b**

R = Pr^n (**c**), Ph (**d**)

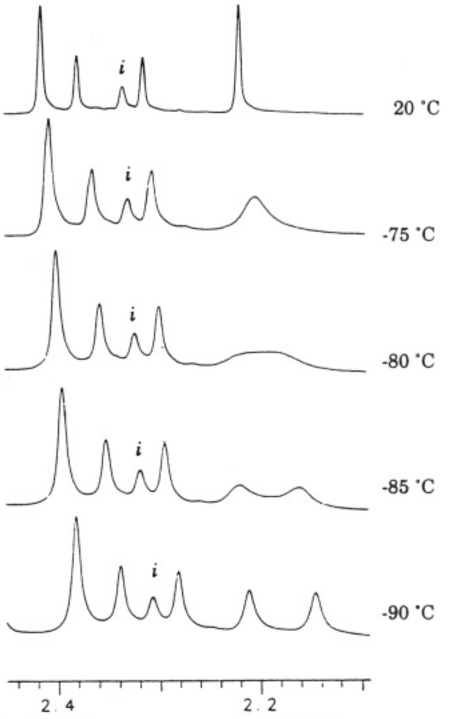

Figure 9. Variable temperature ^1H NMR spectra of the Tp′ methyl signals of $Tp'(CO)_2W(N{=}CHPr^n)$ (**7a**) in CD_2Cl_2 (*i* denotes impurities).

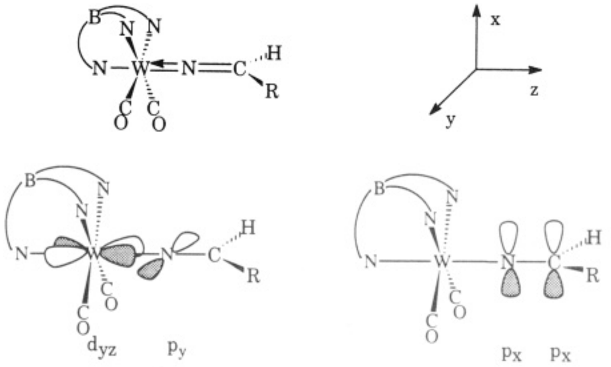

Figure 10. Drawings of the metal dπ–nitrogen pπ and nitrogen pπ–carbon pπ interactions for $Tp'(CO)_2W(N{=}CHR)$ (**7a,b**).

These azavinylidene complexes (**7a,b**) appear to have a plane of symmetry at room temperature, as judged by ^1H and ^{13}C NMR spectroscopy. The pyrazole ring protons of the Tp′ ligand show two sets of resonances in a 2:1 ratio, and the two carbonyl ligands exhibit a single ^{13}C resonance (the 18 protons of the six methyl groups of the Tp′ ligand appear in a 6:3:3:6 ratio). Low temperature ^1H NMR experiments with **7a** suggest that this apparent mirror plane is caused by rapid rotation around the WNC axis. As **7a** is cooled, the signal at 2.20 ppm, which integrates for six protons (two equivalent CH_3 groups of Tp′), broadens until the coalescence temperature (−80 °C) is reached (Figure 9). Upon further cooling, two distinct resonances, each integrating for three protons, at 2.21 and 2.14 ppm, are observed ((6:3:3:3:3) pattern for the six Tp′ methyls). $\Delta G^{\ddagger}$ for this process is 9.6 kcal/mol. At low temperatures the rate of rotation of the WNC unit is no longer rapid on the NMR time scale, and the HCR plane aligns itself perpendicular to the plane that bisects the Tp′ ligand and the two carbonyl ligands (Figure 10). Consequently, the molecule has overall C_1 symmetry.

Here, as in the amido complexes $[Tp'(CO)_2W(N(R)R')$ (**1a–e** and **4a–c**)], maximal π orbital interaction occurs when the p$_y$ orbital of nitrogen interacts with the tungsten d$_{yz}$ orbital (Figure 10). Because the WN and NC π systems are necessarily orthogonal, the HCR fragment is expected to lie orthogonal to the $Tp'(CO)_2W$ mirror plane, i.e. in the *yz* plane. In a similar low temperature ^1H NMR experiment with **7b**, significant broadening is observed for one of the Tp′ methyl signals although the coalescence temperature is not reached even at −105 °C. Low barriers

---

[31] Recent publications on azavinylidene complexes: (a) Daniel, T.; Müller, M.; Werner, H. *Inorg. Chem.* **1991**, *30*, 3118 and ref 2 therein. (b) Feng, S. G.; Templeton, J. L. *J. Am. Chem. Soc.* **1989**, *111*, 6477. (c) Feng, S. G.; White, P. S.; Templeton, J. L. *Organometallics* **1993**, *12*, 1765. (d) Feng, S. G.; White, P. S.; Templeton, J. L. *Organometallics* **1993**, *12*, 2131.

[32] (a) Chatt, J.; Dosser, J.; Leigh, G. J. *J. Chem. Soc., Chem. Commun.* **1972**, 1243. (b) Hughes, D. L.; Ibrahim, S. K.; Macdonald, C. J.; Ali, H. M.; Pickett, C. J. *J. Chem. Soc., Chem. Commun.* **1992**, 1762.

[33] (a) Farmery, K.; Kilner, M.; Midcalf, C. *J. Chem. Soc. A* **1970**, 2279. (b) Bercaw, J. E.; Davies, D. L.; Wolczanski, P. T. *Organometallics* **1986**, *5*, 443. (c) Erker, G.; Frömberg, W.; Atwood, J. L.; Hunter, W. E. *Angew. Chem., Int. Ed. Engl.* **1984**, *23*, 68.

Scheme 1

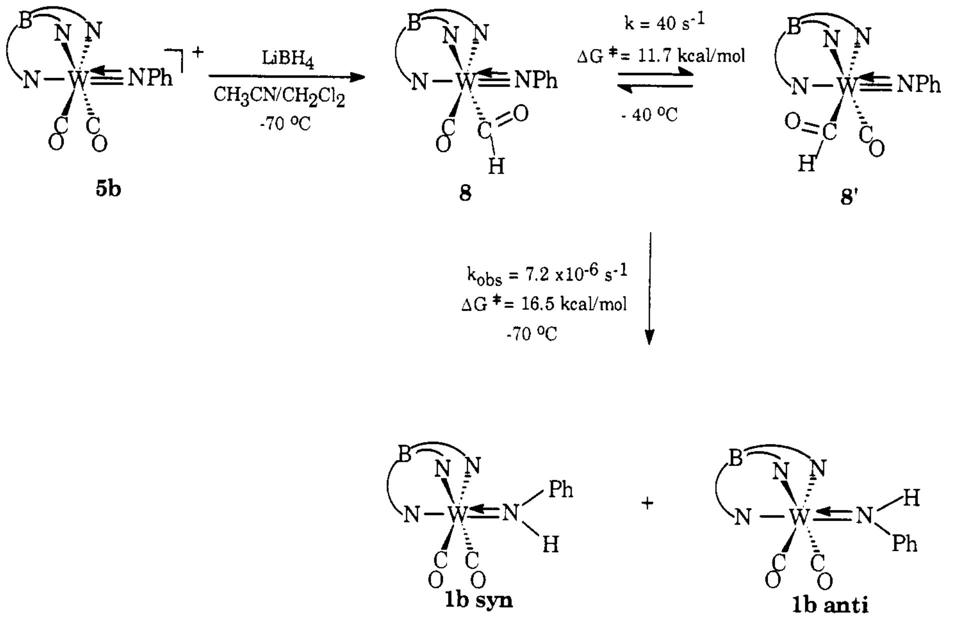

to rotation have been reported for other azavinylidene complexes.[34]

An indication of the electrophilic nature of the nitrene nitrogen in [Tp′(CO)$_2$W(NR)][PF$_6$] is the formation of Tp′(CO)$_2$W(NHR) [R = Bu^t (**1a**) and R = Ph (**1b**)] on addition of LiBH$_4$ to [Tp′(CO)$_2$W(NR)][PF$_6$] (**5a** and **5b**, respectively) (eq 10). Mechanistic studies carried out at

$$[\mathrm{Tp'(CO)_2W{\equiv}NR}][\mathrm{PF_6}] \xrightarrow[\mathrm{CH_3CN}]{\mathrm{LiBH_4}} \mathrm{Tp'(CO)_2W{=}N(H)R} \qquad (10)$$

5a, **5b** → **1a**, **1b**

R = Bu^t (**a**), Ph (**b**)

low temperature (−70 °C) with [Tp′(CO)$_2$W(NPh)][PF$_6$] (**5b**) indicate that hydride initially attacks at a carbonyl carbon to form a formyl complex, Tp′(CO)(C(O)H)W(NPh) (**8**), which then undergoes hydride migration to nitrogen (Scheme 1). The formyl intermediate (**8**) is characterized by C_1 symmetry which is reflected in the 1:1:1 pattern for the three pyrazole protons of the Tp′ ligand in the ^{1}H NMR spectrum at −70 °C. The formyl hydrogen appears at 16.5 ppm (in CD$_3$CN) and is strongly coupled to tungsten ($^2J_{WH}$ = 20 Hz).[35] The terminal carbonyl and formyl carbons are located at 259 and 293 ppm ($^1J_{HC}$ = 132 Hz), respectively.[35] The terminal carbonyl is evident in the infrared spectrum as a strong absorption at 1948 cm^{-1}, while a weak absorption at 1680 cm^{-1} is assigned to the formyl carbonyl.[35] When this formyl complex is warmed from −70 °C, fluxional behavior is observed, as two of the three pyrazole proton signals broaden in the ^{1}H NMR spectrum. At −41 °C these signals coalesce and lead to a rate constant for site exchange of 40 s^{-1}, corresponding to $\Delta G^‡$ = 11.7 kcal/mol. This fluxional behavior is attributed to degenerate hydride migration from the formyl to the carbonyl ligand, **8** ⇌ **8′**.

At low temperature (−70 °C) the rate of hydride migration from carbon to nitrogen is determined to be first order (k_{obs} = 7.2 × 10^{-6} s^{-1}, $\Delta G^‡$ = 16.5 kcal/mol), and the 1:1 ratio of the syn and anti isomers of Tp′(CO)$_2$W(NHPh) (**1b**) represents the kinetically controlled ratio since the interconversion of these isomers at this temperature is exceedingly slow (from the rate data for interconversion (see above) the $t_{1/2}$ can be estimated as greater than 10^7 days). This hydride migration from carbon to nitrogen has been determined to be intramolecular by crossover experiments which are described in detail in a previous communication.[26b] Although this reaction occurs by initial attack of the hydride reagent at the carbonyl ligand, the net reaction is, nevertheless, addition of hydride at nitrogen and provides one example of an electrophilic nitrene ligand.

Synthesis and Reactivity of Tp′(CO)$_2$WN (9). Deprotonation of the parent nitrene complex, [Tp′(CO)$_2$W(NH)][PF$_6$] (**6a**), with Et$_3$N or KH leads to the formation of a new dicarbonyl species with carbonyl stretching frequencies at 2041 and 1944 cm^{-1}. By ^{1}H NMR spectroscopy the characteristic 2:1 pattern for the protons of the three pyrazole rings of the Tp′ ligand indicates the presence of a mirror plane. Although this complex has not been isolated, spectroscopic data are consistent with formation of the neutral nitrido complex, Tp′(CO)$_2$WN (**9**) (eq 11).[36] The d^2 configuration in this complex and,

$$[\mathrm{Tp'(CO)_2W{\equiv}NH}]^+ \xrightarrow{\mathrm{Et_3N\ or\ KN}} \mathrm{Tp'(CO)_2W{\equiv}N{:}} \qquad (11)$$

6a → **9**

consequently, the metal dπ interactions with the nitrogen pπ orbitals are analogous to those of the linear cationic nitrene complexes (vide supra; Figure 7, R = lone pair). The product of the reaction of Tp′(CO)$_2$WI with [(Ph$_3$P)$_2$N][N$_3$] at low temperature appears spectroscopically to be identical to **9** (eq 12). This synthesis provides a direct route to **9** and supplied ample material for reactivity studies.

---

[34] (a) Erker, G.; Frömberg, W.; Krüger, C.; Raabe, E. *J. Am. Chem. Soc.* **1988**, *110*, 2400. (b) Dormond, A.; Aaliti, A.; Elbouadili, A.; Moise, C. *J. Organomet. Chem.* **1987**, *329*, 187.

[35] (a) Casey, C. P.; Andrews, M. A.; Rinz, J. E. *J. Am. Chem. Soc.* **1979**, *101*, 741. (b) Tam, W.; Wong, W.-K.; Gladysz, J. A. *J. Am. Chem. Soc.* **1979**, *101*, 1589. (c) Casey, C. P.; Andrews, M. A.; McAlister, D. R.; Rinz, J. E. *J. Am. Chem. Soc.* **1980**, *102*, 1927. (d) Gladysz, J. A. *Adv. Organomet. Chem.* **1982**, *20*, 1 and references therein.

[36] For structurally characterized nitrido complexes, see: (a) Reference 24c. (b) Groves, J. T.; Takahashi, T.; Butler, W. M. *Inorg. Chem.* **1983**, *22*, 884. (c) Hill, C. L.; Hollander, F. J. *J. Am. Chem. Soc.* **1982**, *104*, 7318.

$$\underset{\mathbf{2}}{Tp'(CO)_2WI} + [(Ph_3P)_2N][N_3] \xrightarrow[CH_2Cl_2]{-78\ ^\circ C} \underset{\mathbf{9}}{Tp'(CO)_2W{\equiv}N:} \quad (12)$$

The nitrido species (**9**) reacts with a variety of electrophiles[37] to yield either dicarbonyl or monocarbonyl imido products. Protonation of **9** with HBF_4 regenerates the parent nitrene (**6a**). Similarly, reaction of **9** with $[Ph_3C][PF_6]$ yields the cationic dicarbonyl triphenylmethyl nitrene (**6b**). Methylation of **9** is effected with MeOTf (Tf = $-SO_2CF_3$) to give $[Tp'(CO)_2W(NMe)][OTf]$ (**10**). Equation 13 summarizes the reactions of **9** with electrophiles to form cationic dicarbonyl nitrene complexes.

$$\underset{\mathbf{9}}{Tp'(CO)_2W{\equiv}N:} \xrightarrow{RX} [Tp'(CO)_2W{\equiv}NR][X] \quad (13)$$

R	X	complex
H	BF_4	**6a**
Ph_3C	PF_6	**6b**
Me	OTf	**10**

Attempts to generate $Tp'(CO)_2WNR^+$ complexes with more strongly electron-withdrawing R groups attached to nitrogen yield instead monocarbonyl products. When **9** is treated with electrophiles such as tosyl chloride, acetyl chloride, or acetic anhydride, only neutral monocarbonyl products, Tp'(CO)(X)W(NR) (R = Ts, X = Cl, **11a**; R = $C(O)CH_3$, X = Cl, **11b**; R = $C(O)CH_3$, X = $OC(O)CH_3$, **11c**) (eq 14), are observed. ^1H and ^{13}C NMR data indicate

$$\underset{\mathbf{9}}{Tp'(CO)_2W{\equiv}N:} \xrightarrow[-CO]{RX} Tp'(CO)(X)W{\equiv}NR \quad (14)$$

R	X	complex
Ts	Cl	**11a**
$-C(O)CH_3$	Cl	**11b**
$-C(O)CH_3$	$-OC(O)CH_3$	**11c**

that the three pyrazole rings of the Tp' ligand are magnetically inequivalent in these complexes. The acetyl carbons ($NC(O)CH_3$) of **11b** and **11c** are strongly coupled to tungsten ($^2J_{W-C}$ = 35 Hz), indicating a nearly linear imido linkage.[30] Elemental analyses of **11a** and **11b** confirm the presence of a chlorine atom in these molecules. X-ray diffraction of a single crystal of **11a** confirms the presence of the chlorine atom in the tungsten coordination sphere and reveals the structure of the tosyl imido ligand. Figure 11 shows an ORTEP diagram of **11a**. The crystallographic data were obtained under the conditions listed in Table 3. The atomic parameters are presented in Table 10. The structure exhibits disorder of the Cl and CO ligands attached to tungsten. This disorder was modeled as 60% Cl/40% CO [Cl(1), O(1)] and 40% Cl/60% CO [Cl(2), O(2)]. Selected bond distances and angles are presented in Table 11. Salient data include the W–N bond distance of 1.78(1) Å, which is indicative of tungsten–nitrogen multiple bonding and the 173(1)° W(1)–N(2)–S(1) bond angle which confirms sp hybridization at nitrogen. Although we do not have data relevant to the mechanism of these reactions, we postulate that the cationic dicarbonyl complexes, $[Tp'(CO)_2W(NR)][X]$, are formed initially. When R is a strong electron-withdrawing group such as tosyl or acetyl and X^- is a more highly coordinating counterion such as chloride or acetate, the metal center is sufficiently electron deficient to render the cationic dicarbonyl complex unstable with respect to displacement of CO by the counterion X^-.

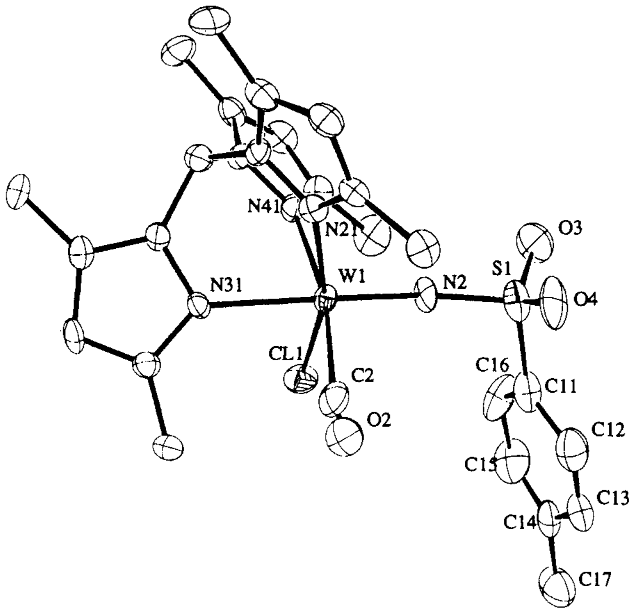

Figure 11. ORTEP diagram of Tp'(CO)ClW(NTs) (**11a**).

Summary

Amido complexes, $Tp'(CO)_2W(NHR)$, have been synthesized and utilized as precursors to both anionic, $Tp'(CO)_2W(NR)^-$, and cationic, $Tp'(CO)_2W(NR)^+$, dicarbonyl tungsten nitrene complexes. The anionic imido complexes, $Tp'(CO)_2W(NR)^-$, react with alkylating agents to give dialkylamido complexes, $Tp'(CO)_2W(NRR')$. $Tp'(CO)_2W(NCH_2R)^+$ complexes can be deprotonated with Et_3N to give neutral azavinylidene complexes, $Tp'(CO)_2W(N{=}CHR)$. Low temperature NMR studies of the reaction of $LiBH_4$ with $Tp'(CO)_2W(NPh)^+$ indicated that the hydride reagent initially attacks at a carbonyl carbon to form a formyl complex, Tp'(CO)(CHO)W(NPh), which then undergoes intramolecular hydride migration from the formyl carbon to nitrogen to form the amido complex, $Tp'(CO)_2W(NHPh)$. The nitrido complex, $Tp'(CO)_2WN$, was synthesized by deprotonation of the parent cationic nitrene complex, $Tp'(CO)_2W(NH)^+$, and also by reaction of $Tp'(CO)_2WI$ with $[(Ph_3P)][N_3]$. This nitrido species reacts with electrophiles (RX) to give both cationic, $[Tp'(CO)_2W(NR)][X]$, and neutral, Tp'(CO)XW(NR), nitrene complexes.

Experimental Section

Materials and Methods. All manipulations were carried out under a dry nitrogen atmosphere with standard Schlenk techniques. Solvents were dried and distilled under nitrogen by standard methods.[38] Literature methods were used to prepare $Tp'(CO)_3WI$,[39] $Tp'(CO)_2WI$,[40] and $[(Ph_3P)_2N][N_3]$.[41] All other reagents were used as obtained from commercial sources.

---

(37) For examples of addition of electrophiles to terminal nitride units, see: (a) Bevan, P. C.; Chatt, J.; Dilworth, J. R.; Henderson, R. A.; Leigh, G. J. *J. Chem. Soc., Dalton Trans.* **1982**, 821. (b) Reference 32b.

(38) Gordon, A. J.; Ford, R. A. *The Chemist's Companion*; Wiley: New York, 1972.

(39) Feng, S. G.; Philipp, C. C.; Gamble, A. S.; White, P. S.; Templeton, J. L. *Organometallics* **1991**, *10*, 3504.

(40) (a) Reference 26c. (b) Philipp, C. C.; Young, C. G.; White, P. S.; Templeton, J. L. *Inorg. Chem.* **1993**, *32*, 5437.

(41) Martinsen, A.; Songstad, J. *Acta Chem. Scand.* **1977**, *A31*, 645.

Table 2. Selected[a] NMR Data[b,c] for Complexes 1a–e, 4a–c, 5a–d, 6a,b, 7a,b, 10, and 11a–c

		^{13}C	
complex	^{1}H	W–*C*O	others
1a, Tp′(CO)$_2$W(NHBu^t)	14.15 (1), br s, N*H* 1.39 (9), s, C(C*H*$_3$)$_3$	255.6 (2) $^1J_{\mathrm{W-C}}$ = 176 Hz	70.5 (1), *C*(CH$_3$)$_3$ 32.2 (3), C(*C*H$_3$)$_3$
1b, Tp′(CO)$_2$W(NHPh)	15.33, br s, N*H*, major isomer 13.0, br s, N*H*, minor isomer isomer ratio 7.5:1 (1) *d*	255.6 (2) $^1J_{\mathrm{W-C}}$ = 173 Hz	161.3 (1), ipso, Ph *d*
1c, Tp′(CO)$_2$W(NHBu^n)	13.7, br t, N*H*, major isomer; $^3J_{\mathrm{H-H}}$ = 8 Hz 11.9, br t, N*H*, minor isomer isomer ratio 6:1 (1) 3.40 (2), dt, C*H*$_2$Pr^n; $^3J_{\mathrm{H-H}}$ = 8 Hz, $^3J_{\mathrm{H-H}}$ = 8 Hz *e*	254.6 (2) $^1J_{\mathrm{W-C}}$ = 177 Hz	73.5 (1), *C*H$_2$Pr^n *e*
1d, Tp′(CO)$_2$W(NHCH$_2$Ph)	13.57, t, N*H*, major isomer; $^3J_{\mathrm{H-H}}$ = 8 Hz 11.82, br t, N*H*, minor isomer isomer ratio 6:1 (1) 4.47 (2), d, NC*H*$_2$Ph; $^3J_{\mathrm{W-H}}$ = 50 Hz, $^3J_{\mathrm{H-H}}$ = 8 Hz *d*	254.7 (2) $^1J_{\mathrm{W-C}}$ = 174 Hz	78.4 (1) N*C*H$_2$Ph *d*
1e, Tp′(CO)$_2$W(NH$_2$)	13.50 (1), br s 11.60 (1), br s	254.7 (2) $^1J_{\mathrm{W-C}}$ = 175 Hz	
4a, Tp′(CO)$_2$W(N(Ph)CH$_2$Ph)	4.42 (2), s, NC*H*$_2$Ph *d*	254.1 (2) $^1J_{\mathrm{W-C}}$ = 178 Hz	78.7 (1), N*C*H$_2$Ph *d*
4b, Tp′(CO)$_2$W(N(Me)CH$_2$Ph)	2.07 (3), N*Me* 4.75 (2), NC*H*$_2$Ph *d*	254.7 (2) $^1J_{\mathrm{W-C}}$ = 175 Hz	57.2 (1), N*C*H$_3$ 87.6 (1), N*C*H$_2$Ph *d*
4c, Tp′(CO)$_2$W(NMe$_2$)	3.30 (3), *Me* 2.16 (3), *Me*	254.8 (2) $^1J_{\mathrm{W-C}}$ = 177 Hz	70.6 (1), *Me* 61.4 (1), *Me*
5a, [Tp′(CO)$_2$W(NBu^t)][PF$_6$]	1.59 (9), s, C(C*H*$_3$)$_3$	216.6 (2) $^1J_{\mathrm{W-C}}$ = 157 Hz	74.0 (1), *C*(CH$_3$)$_3$; $^2J_{\mathrm{W-C}}$ = 23 Hz 30.6 (3), C(*C*H$_3$)$_3$
5b, [Tp′(CO)$_2$W(NPh)][PF$_6$]	7.50 (5), m, N*Ph*	216.9 (2) $^1J_{\mathrm{W-C}}$ = 153 hz	153.6, ipso, Ph; $^2J_{\mathrm{W-C}}$ = 31 Hz *d*
5c, [Tp′(CO)$_2$W(NBu^n)][PF$_6$]	3.77 (2), t, NC*H*$_2$Pr^n; $^3J_{\mathrm{H-H}}$ = 8 Hz *e*	216.8 (2) $^1J_{\mathrm{W-C}}$ = 158 Hz	67.5 (1), N*C*H$_2$Pr^n; $^2J_{\mathrm{W-C}}$ = 26 Hz *e*
5d, [Tp′(CO)$_2$W(NCH$_2$Ph)][PF$_6$]	4.81 (2), NC*H*$_2$Ph; $^3J_{\mathrm{W-H}}$ = 8 Hz *d*	216.0 (2) $^1J_{\mathrm{W-C}}$ = 155 Hz	71.9 (1), N*C*H$_2$Ph; $^2J_{\mathrm{W-C}}$a = 27 Hz *d*
6a, [Tp′(CO)$_2$W(NH)][PF$_6$]	9.8 (1), br, N*H*	215.6 (2) $^1J_{\mathrm{W-C}}$ = 159 Hz	
6b, [Tp′(CO)$_2$W(NCPh$_3$)][PF$_6$]	*d*	219.3 (2) $^1J_{\mathrm{W-C}}$ = 158 Hz	93.3 *C*Ph$_3$ *d*
7a, Tp′(CO)$_2$W(N═CHPr^n)	3.02 (1), t, NC*H*Pr^n; $^3J_{\mathrm{H-H}}$ = 6 Hz $^3J_{\mathrm{W-H}}$ = 6 Hz *e*	241.7 (2) $^1J_{\mathrm{W-C}}$ = 174 Hz	150.0 (1), N*C*HPr^n; $^2J_{\mathrm{W-C}}$ = 27 Hz *e*
7b, Tp′(CO)$_2$W(N—CHPh)	3.79 (1), NC*H*Ph; $^3J_{\mathrm{W-H}}$ = 4 Hz *d*	239.1 (2) $^1J_{\mathrm{W-C}}$ = 171 Hz	147.3 (1), N*C*HPh; $^2J_{\mathrm{W-C}}$ = 26 Hz *d*
10, [Tp′(CO)$_2$W(NMe)][PF$_6$]	3.67 (3), *Me*; $^3J_{\mathrm{W-H}}$ = 10 Hz	216.6 (2)	55.9 (1), *Me*
11a, Tp′(CO)ClW(NTs)	Ts (AA′XX′ spin system) δA, 7.77 (2); δX, 7.36 (2); $J_{\mathrm{appH-H}}$ = 8 Hz *g* (3), *p-Me* (Ts)	279.8 (1)	*f*
11b, Tp′(CO)ClW(NC(O)CH$_3$)	1.73 (3), NC(O)C*H*$_3$	280.6 (1) $^1J_{\mathrm{W-C}}$ = 177 Hz	180.9 (1), N*C*OCH$_3$; $^2J_{\mathrm{W-C}}$ = 35 Hz 31.9 (1), NCO*C*H$_3$
11c, Tp′(CO)(OC(O)CH$_3$)W(NC(O)CH$_3$)	*g* (3), NC(O)C*H*$_3$ *g* (3), OC(O)C*H*$_3$	284.8 (1) $^1J_{\mathrm{W-C}}$ = 185 Hz	181.7 (1), N*C*OCH$_3$; $^2J_{\mathrm{W-C}}$ = 35 Hz 175.7 (1), O*C*OCH$_3$ 24.4 (1), NCO*C*H$_3$ or OCO*C*H$_3$ 23.2 (1), NCO*C*H$_3$ or OCO*C*H$_3$

[a] ^{1}H and ^{13}C{^{1}H} Tp′ resonances are reported in the Experimental Section. [b] In ppm. Intensities in parentheses. [c] Deuterated solvents used: C$_6$D$_6$ for **11b** and **11c**; CD$_2$Cl$_2$ for all other complexes. [d] Phenyl resonances are reported in the Experimental Section. [e] Propyl resonances are reported in the Experimental Section. [f] Tosyl resonances are reported in the Experimental Section. [g] This resonance is found in the same range as the Tp′ Me resonances and is reported in the Experimental Section.

Infrared spectra were obtained with a Mattson Polaris Fourier transform spectrophotometer. ^{1}H NMR were recorded on a Bruker AC200, Bruker WM250, or Varlian XL400 instrument. ^{13}C NMR spectra were obtained on a Varian XL400 instrument. Elemental analyses were performed by Atlantic Microlab Inc. of Norcross, GA, Galbraith Laboratories of Knoxville, TN, or Oneida Research Services of Whitesboro, NY.

Tp′(CO)$_2$W(NHR) [R = Bu^t, 1a; R = Ph, 1b]. Method A. A 4-fold excess of the corresponding amine (NH$_2$R) was added to 100 mL of a dark red THF solution of Tp′(CO)$_3$WI (2.00 g, 2.9 mmol). The solution was heated at reflux for 3–4 h. Volatiles were removed in vacuo, and the residue was chromatographed on an alumina (80–200 mesh) column. Following elution with toluene, crystallization from CH$_2$Cl$_2$/Et$_2$O (R = Bu^t) or toluene (R = Ph) afforded complex **1a** as aqua blue crystals or **1b** as yellow crystals in 81% or 88% yield, respectively.

Method B. A 4-fold excess of the corresponding amine (NH$_2$R) was added to 100 mL of a yellow CH$_2$Cl$_2$ solution of Tp′(CO)$_2$WI (**2**) (1.00 g, 1.5 mmol). After stirring 15 min (**1a**) or 0.5 h (**1b**), the solution was reduced to dryness. The residue was chromatographed on an alumina (80–200 mesh) column. Following elution with toluene, crystallization from CH$_2$Cl$_2$/Et$_2$O (R = Bu^t) or toluene (R = Ph) afforded complex **1a** as aqua blue crystals or **1b** as yellow crystals in 60% or 95% yield, respectively. Data for **1a**: ^{1}H NMR (CD$_2$Cl$_2$, δ) 14.15 [1H, s, N*H*], 5.93, 5.88 [3H (1:2), 3 C*H*'s of Tp′], 2.50, 2.43, 2.36, 2.01 [18H (6:3:3:6), 6 C*H*$_3$'s

Table 3. Crystallographic Data for Tp′(CO)$_2$W(N(Ph)CH$_2$Ph) (4a), Tp′(CO)$_2$W(NMe$_2$) (4c), [Tp′(CO)$_2$W(NPh)][PF$_6$] (5b), and Tp′(CO)ClW(NTs) (11a)

complex	**4a**·CH_2Cl_2	**4c**	**5b**	**11a**
formula	$BC_{31}ClH_{36}N_7O_2W$	$BC_{19}H_{28}N_7O_2W$	$BC_{23}F_6H_{27}N_7O_2PW$	$BC_{23}ClH_{29}N_7O_3SW$
mol wt	804.23	581.13	773.13	713.70
cryst syst	triclinic	triclinic	monoclinic	monoclinic
space group	$P\bar{1}$	$P\bar{1}$	$P2_1/n$	$P2_1$
a, Å	11.452(2)	11.151(4)	10.301(2)	8.222(3)
b, Å	11.597(2)	11.702(3)	10.389(2)	17.256(6)
c, Å	14.144(2)	10.391(4)	27.816(7)	9.561(4)
α, deg	86.78(1)	93.46(3)		
β, deg	84.41(1)	108.56(3)	97.69(2)	100.85(3)
γ, deg	64.37(1)	63.20(3)		
V, Å^3	1685.4(4)	1141.7(7)	2950.1(1)	1332.3(8)
Z	2	2	4	2
D_{calc}, g cm^{-3}	1.585	1.690	1.741	1.761
$F(000)$	798.55	569.97	1507.55	697.78
cryst dimens, mm	0.25 × 0.25 × 0.30	0.25 × 0.25 × 0.15	0.40 × 0.20 × 0.20	0.30 × 0.30 × 0.30
temp, °C	20	20	20	20
radiation, Å	Mo K$\bar{\alpha}$ (0.710 73)	Mo K$\bar{\alpha}$ (0.710 73)	Mo K$\bar{\alpha}$ (0.710 73)	Mo K$\bar{\alpha}$ (0.710 73)
2θ range, deg	$5 < 2\theta < 45$	$5 < 2\theta < 55$	$5 < 2\theta < 45$	$5 < 2\theta < 50$
μ, mm^{-1}	3.70	5.19	4.12	4.55
scan mode	$\theta/2\theta$	$\theta/2\theta$	$\theta/2\theta$	$\theta/2\theta$
no. of data collected	(−11,0,−15) to (12,12,15)	(−12,0,−13) to (14,15,13)	(−11,0,0) to (10,11,29)	(−9,0,0) to (9,20,11)
total no. of data	5015	5541	3827	3573
total no. of unique data	4399	5274	3827	3497
no. of obs data ($I > 2.5\sigma(I)$)	3910	4208	2885	2985
R_F	0.037	0.039	0.036	0.040
R_w	0.046	0.043	0.045	0.046
GoF	1.66	1.25	1.49	1.52

of Tp′], 1.39 [9H, s, C(CH_3)$_3$]; ^{13}C NMR (CD_2Cl_2, δ) 255.6 [$^1J_{WC}$ = 176 Hz, 2 *C*O], 160.0, 152.3, 146.7, 145.5, [(1:2:1:2), 6 *C*CH$_3$ of Tp′], 108.5, 106.8 [(1:2), 3 *C*H of Tp′], 70.5 [1 *C*(CH$_3$)$_3$], 32.2 [3 C(*C*H$_3$)$_3$], 18.0, 16.4, 13.1, 12.7 [(2:1:1:2), 6 *C*H$_3$'s of Tp′]. Anal. Calcd for **1a**: C, 41.40; H, 5.29; N, 16.09. Found: C, 41.14; H, 5.43; N, 15.90. Data for **1b**: ^{1}H NMR (CD_2Cl_2, δ) (major isomer except where noted) 15.33, 13.0 [two br s (7.5:1), which together account for 1H, major and minor isomer N*H*], 7.30 (5H, m, Ph), 6.09, 5.90 [3H (1:2), 3 C*H*'s of Tp′], 2.60, 2.52, 2.45, 1.80 [18H (6:3:3:6), 6 C*H*$_3$'s of Tp′]; ^{13}C NMR (CD_2Cl_2, δ) (major isomer) 255.6 [$^1J_{WC}$ = 173 Hz, 2 *C*O] 161.3 (ipso C of Ph), 161.2, 152.3, 147.8, 145.4 [(1:2:1:2), 6 *C*CH$_3$ of Tp′], 129.4, 128.5 (ortho and meta C of Ph), 125.6 (para C of Ph), 109.2, 106.9 [(1:2), 3 *C*H of Tp′], 17.1, 16.9, 13.2, 12.6 [(1:2:1:2), 6 *C*H$_3$'s of Tp′]. Anal. Calcd for **1b**·PhCH$_3$ [$WC_{23}H_{28}BN_7O_2$]: C, 50.02; H, 5.04; N, 13.61. Found: C, 49.72; H, 5.07; N, 13.06.

Tp′(CO)$_2$W(NHBu^n) (1c). Excess NH$_2$Bu^n (0.65 mL, 6.0 mmol) was added to 100 mL of a yellow THF solution of Tp′(CO)$_2$WI (1.00 g, 1.5 mmol). The resulting blue solution was stirred for 15 min. Volatiles were removed in vacuo, and the residue was washed with MeOH (2 × 30 mL). The blue solid which remained was recrystallized from a 1:1 mixture of toluene/MeOH to yield crystalline **1c** (0.54 g, 60%). ^{1}H NMR (CD_2Cl_2), major isomer except where noted: 13.7, 11.9 [two br t, $^3J_{HH}$ = 8 Hz, (6:1) which together accounted for 1H, major and minor isomer N*H*], 5.99, 5.88 [3H (1:2), 3 C*H*'s of Tp′], 3.40 [2H, q, $^3J_{HH}$ = 8 Hz, $^3J_{HH}$ = 8 Hz, C*H*$_2$CH$_2$CH$_2$CH$_3$], 2.51, 2.44, 2.40, 2.01 [18H (6:3:3:6), 6 C*H*$_3$'s of Tp′], 1.65 (2H, m, CH$_2$C*H*$_2$CH$_2$CH$_3$), 1.40 (2H, m, CH$_2$CH$_2$C*H*$_2$CH$_3$), 0.96 (3H, t, $^3J_{H-H}$ = 7 Hz, C*H*$_3$). ^{13}C NMR (CD_2Cl_2, δ), major isomer: 254.6 ($^1J_{WC}$ = 177 Hz, 2 *C*O), 160.1, 152.0, 147.0, 145.2 [(1:2:1:2), 6 *C*CH$_3$ of Tp′], 108.6, 106.8 [(1:2), 3 *C*H of Tp′], 73.5 (*C*H$_2$CH$_2$CH$_2$CH$_3$), 17.5, 16.8, 13.1, 12.6 [(2:1:1:2), 6 *C*H$_3$'s of Tp′], 34.9 (CH$_2$*C*H$_2$CH$_2$CH$_3$), 20.6 (CH$_2$CH$_2$*C*H$_2$CH$_3$), 14.2 (1 *C*H$_3$ of Bu^n)]. Anal. Calcd for **1c**: C, 41.40; H, 5.29; N, 16.09. Found: C, 40.34; H, 5.21; N, 15.89.

Tp′(CO)$_2$W(NHCH$_2$Ph) (1d). Benzylamine (2.20 g, 20 mmol) was added to a solution of Tp′(CO)$_2$WI (**2**) (4.40 g, 6.7 mmol) in CH_2Cl_2 (50 mL). The original orange color of the solution immediately turned blue-green. The solvent was then removed in vacuo; a green oil remained. EtOH (50 mL) was added and the mixture was stirred for 1 h before filtering to yield a blue powder. This powder was washed with an additional 50 mL of EtOH and recrystallized from a 2:1 hexanes:CH_2Cl_2 mixture. Yield: 75%. ^{1}H NMR (CD_2Cl_2, δ), major isomer except where noted: 13.57, 11.82 [two br t, $^3J_{HH}$ = 8 Hz, (6:1) which together account for 1H, major and minor isomer N*H*], 5.99, 5.81 [3H (1:2), 3 C*H*'s of Tp′], 4.47 (2H, d, $^3J_{HH}$ = 8 Hz, $^3J_{WH}$ = 50 Hz, C*H*$_2$Ph), 2.46, 2.45, 2.37, 1.74 [18H (6:3:3:6), 6 C*H*$_3$'s of Tp′], 7.4–7.1 (5H, m, Ph). ^{13}C NMR (CD_2Cl_2, δ), major isomer: 254.7 ($^1J_{WC}$ = 174 Hz, 2 *C*O), 160.1, 152.0, 147.1, 145.1 [(1:2:1:2), 6 *C*CH$_3$ of Tp′], 140.6 (ipso C of Ph), 129.2 (ortho C of Ph), 129.0 (meta C of Ph), 127.5 (para C of Ph), 108.6, 106.7 [(1:2), 3 *C*H of Tp′], 78.4 (*C*H$_2$Ph), 17.1, 16.8, 13.0, 12.5 [(2:1:1:2), 6 *C*H$_3$'s of Tp′]. Anal. Calcd for **1d**: C, 44.82; H, 4.70; N, 15.24. Found: C, 44.18; H, 4.64; N, 14.90.

Tp′(CO)$_2$W(NH$_2$) (1e). Ammonia was bubbled through a solution of complex **2** (2.00 g, 3.0 mmol) in CH_2Cl_2 (50 mL) at −50 °C for 5 min. The initial orange solution color changed to blue-green. Volatiles were removed in vacuo, and the residue was washed with EtOH (2 × 50 mL) and Et$_2$O (2 × 50 mL). The resulting green solid (**1e**) was suitable for further reactions. Attempts to obtain an analytical sample resulted in decomposition. Yield: 55%. ^{1}H NMR (CD_2Cl_2, δ): 13.50 (1H, s, br, N*H*H′), 11.60 (1H, s, br, NH*H′*), 6.06, 5.90 [3H (1:2), 3 C*H*'s of Tp′], 2.53, 2.48, 2.41, 2.00 [18H (6:3:3:6), 6 C*H*$_3$'s of Tp′]. ^{13}C NMR (CD_2Cl_2, δ): 254.7 ($^1J_{WC}$ = 175 Hz, 2 *C*O), 160.8, 151.6, 147.3, 145.0 [(1:2:1:2), 6 *C*CH$_3$ of Tp′], 108.9, 106.6 [(1:2), 3 *C*H of Tp′], 17.7, 16.9, 13.1, 12.5 [(2:1:1:2), 6 *C*H$_3$'s of Tp′].

Tp′(CO)$_2$W(N(Ph)CH$_2$Ph) (4a). Excess Bu^{t}Li (2.20 mL, 5.5 mmol) in hexane solution was added to 100 mL of a yellow THF solution of Tp′(CO)$_2$W(NHPh) (**1b**) (1.18 g, 1.9 mmol) at −78 °C. The solution color immediatedly turned burgundy. Excess benzyl bromide (0.5 mL, 3.0 mmol) was then added, and after standing at −78 °C for 1 h, the reaction mixture was warmed to room temperature. The solvent was evaporated, and the residue was chromatographed on an alumina (80–200-mesh) column. A 1:1 mixture of CH_2Cl_2 and hexane eluted a green band. The product was isolated as green crystals (1.08 g, 80%) upon recrystallization by slow diffusion of a CH_2Cl_2 solution into hexane. ^{1}H NMR (CD_2Cl_2, δ): 7.10 (10H, m, 2 Ph), 5.96, 5.93 [3H (2:1), 3 C*H*'s of Tp′], 4.42 (2H, s, C*H*$_2$Ph), 2.62, 2.36, 2.34, 1.93 [18H (6:3:3:6), 6 C*H*$_3$'s of Tp′]. ^{13}C NMR (CD_2Cl_2, δ): 254.1 ($^1J_{WC}$ = 178 Hz, 2 *C*O), 167.8 (ipso C of N*Ph*), 160.4, 152.5, 146.7, 146.2 [(1:2:1:2), 6 *C*CH$_3$ of Tp′], 135.7 (ipso C of CH$_2$*Ph*), 130.1, 128.2, 127.7, 123.1 [(2:2:2:2), 8 C ortho and meta of 2 Ph], 127.2, 124.8 (2 C para of 2 *Ph*), 108.4, 107.2 [(1:2), 3 *C*H of Tp′], 78.7 (*C*H$_2$Ph), 16.5, 16.4, 13.0, 12.8 [(2:1:1:2), 6 *C*H$_3$'s of Tp′]. Anal. Calcd for

Table 4. Atomic Positional Parameters for $Tp'(CO)_2W(N(Ph)CH_2Ph)\cdot CH_2Cl_2$ 4a·CH_2Cl_2)

atom	x	y	z	B_{iso}, Å^2
W(1)	0.12537(3)	0.20820(3)	0.19089(2)	3.13(1)
C(1)	–0.0335(7)	0.2229(7)	0.1429(5)	4.3(4)
O(1)	–0.1268(5)	0.2181(6)	0.1187(4)	6.1(4)
C(2)	0.1334(7)	0.0371(8)	0.2018(5)	4.7(4)
O(2)	0.1297(7)	–0.0635(5)	0.2035(5)	6.7(4)
N(3)	0.0342(5)	0.2734(5)	0.3165(4)	3.5(3)
C(4)	0.0568(7)	0.3687(7)	0.3699(5)	4.2(4)
C(11)	0.1100(8)	0.3226(7)	0.4646(6)	5.0(4)
C(12)	0.2335(9)	0.302(1)	0.4782(8)	7.8(6)
C(13)	0.284(1)	0.261(1)	0.565(1)	11.3(9)
C(14)	0.214(2)	0.2353(1)	0.6382(9)	12(1)
C(15)	0.093(2)	0.256(1)	0.6277(7)	10(1)
C(16)	0.037(1)	0.302(1)	0.5408(6)	6.9(6)
C(21)	–0.0729(7)	0.2514(6)	0.3618(5)	3.5(3)
C(22)	–0.0552(8)	0.1288(8)	0.3889(5)	4.9(4)
C(23)	–0.1583(9)	0.1060(8)	0.4299(6)	5.4(5)
C(24)	–0.2784(8)	0.2032(9)	0.4452(6)	5.7(5)
C(25)	–0.2976(8)	0.329(1)	0.4206(6)	6.2(5)
C(26)	–0.1962(7)	0.3507(7)	0.3767(5)	4.7(4)
B(1)	0.3516(8)	0.2976(8)	0.1011(6)	4.0(4)
N(31)	0.3192(5)	0.1670(5)	0.2407(4)	3.5(3)
N(32)	0.3918(5)	0.2272(5)	0.1959(4)	3.7(3)
C(33)	0.5028(6)	0.1894(7)	0.2388(5)	3.7(4)
C(34)	0.5015(7)	0.1065(7)	0.3109(5)	4.0(3)
C(35)	0.3877(7)	0.0939(7)	0.3103(5)	3.8(4)
C(36)	0.6049(7)	0.2341(9)	0.2068(6)	5.4(5)
C(37)	0.3406(8)	0.0128(8)	0.3732(6)	5.2(5)
N(41)	0.1112(5)	0.4012(5)	0.1449(4)	3.6(3)
N(42)	0.2230(6)	0.4151(5)	0.1142(4)	3.8(3)
C(43)	0.1905(8)	0.5382(7)	0.0880(6)	4.8(4)
C(44)	0.0583(9)	0.6030(7)	0.1014(6)	5.4(5)
C(45)	0.0096(7)	0.5165(6)	0.1362(5)	4.0(3)
C(46)	0.289(1)	0.5866(9)	0.0515(8)	7.2(6)
C(47)	–0.1258(8)	0.5381(7)	0.1574(6)	5.0(4)
N(51)	0.2404(5)	0.1638(5)	0.0532(4)	3.7(3)
N(52)	0.3353(5)	0.2066(5)	0.0332(4)	3.7(3)
C(53)	0.3989(7)	0.1610(7)	–0.0513(5)	4.5(4)
C(54)	0.3445(8)	0.0892(8)	–0.0871(5)	4.8(4)
C(55)	0.2462(7)	0.0933(7)	–0.0206(5)	4.1(4)
C(56)	0.5134(9)	0.1851(9)	–0.0932(6)	6.4(5)
C(57)	0.1550(8)	0.0322(8)	–0.0281(6)	5.2(5)
C(61)	0.321(2)	0.674(1)	0.3160(9)	11.2(10)
Cl(1)	0.4826(4)	0.6419(4)	0.3190(3)	12.3(3)
Cl(2)	0.3041(5)	0.5335(5)	0.3210(4)	14.9(4)

Table 5. Atomic Positional Parameters for $Tp'(CO)_2W(NMe_2)$ (4c)

atom	x	y	z	B_{iso}, Å^2
W(1)	0.42459(3)	0.27945(2)	0.24350(3)	2.84(1)
C(1)	0.4160(8)	0.4497(7)	0.2626(7)	4.2(4)
O(1)	0.4229(6)	0.5457(5)	0.2697(6)	5.9(3)
C(2)	0.5562(7)	0.2875(7)	0.1640(7)	4.1(4)
O(2)	0.6345(6)	0.3013(6)	0.1219(6)	6.3(4)
N(3)	0.5726(6)	0.2053(5)	0.4205(6)	3.9(3)
C(4)	0.6923(8)	0.2317(8)	0.4874(8)	5.5(4)
C(5)	0.5754(9)	0.1067(8)	0.5055(8)	5.3(5)
B(1)	0.1777(8)	0.1798(7)	0.1379(8)	3.7(4)
N(11)	0.2590(5)	0.2957(5)	0.3312(5)	3.4(3)
N(12)	0.1746(5)	0.2380(5)	0.2738(5)	3.4(3)
C(13)	0.0940(7)	0.2488(7)	0.3521(7)	4.1(4)
C(14)	0.1288(8)	0.3141(8)	0.4597(7)	4.8(4)
C(15)	0.2297(7)	0.3448(7)	0.4440(7)	4.0(4)
C(16)	–0.0045(8)	0.1888(8)	0.3229(9)	5.7(5)
C(17)	0.298(1)	0.4173(9)	0.5305(8)	5.8(6)
C(24)	0.5033(9)	–0.1194(7)	0.1567(7)	4.6(4)
C(25)	0.5496(7)	–0.0274(6)	0.1908(6)	3.6(3)
C(26)	0.2564(1)	–0.1122(8)	0.0997(9)	5.8(5)
C(27)	0.6972(8)	–0.0426(7)	0.2219(8)	5.0(4)
N(21)	0.4415(5)	0.0849(5)	0.1943(5)	3.3(3)
N(22)	0.3234(5)	0.0650(5)	0.1584(5)	3.4(3)
C(23)	0.3603(8)	–0.0594(6)	0.1364(7)	4.0(4)
N(31)	0.2437(5)	0.3364(5)	0.0543(5)	3.3(3)
N(32)	0.1532(5)	0.2819(5)	0.0310(5)	3.5(3)
C(33)	0.0544(6)	0.3268(6)	–0.0906(7)	3.8(3)
C(34)	0.0795(7)	0.4132(7)	–0.1503(7)	4.3(4)
C(35)	0.1963(7)	0.4179(6)	–0.0580(7)	3.8(4)
C(36)	–0.0560(8)	0.2832(9)	–0.1501(9)	6.1(5)
C(37)	0.2676(9)	0.4933(7)	–0.0766(8)	5.3(5)

Table 6. Selected Bond Distances (Å) and Angles (deg) for $Tp'(CO)_2W(N(Ph)CH_2Ph)$ (4a)

W(1)–C(1)	1.939(7)	W(1)–N(51)	2.196(5)
W(1)–C(2)	1.944(8)	C(1)–O(1)	1.177(9)
W(1)–N(3)	1.981(6)	C(2)–O(2)	1.184(9)
W(1)–N(31)	2.236(5)	N(3)–C(4)	1.496(8)
W(1)–N(41)	2.237(5)	N(3)–C(21)	1.442(9)
C(1)–W(1)–C(2)	74.6(3)	N(3)–W(1)–N(41)	91.6(2)
C(1)–W(1)–N(3)	91.6(3)	N(3)–W(1)–N(51)	169.0(2)
C(1)–W(1)–N(31)	173.2(3)	N(31)–W(1)–N(41)	87.2(2)
C(1)–W(1)–N(41)	98.2(3)	N(31)–W(1)–N(51)	81.4(2)
C(1)–W(1)–N(51)	95.4(3)	N(41)–W(1)–N(51)	79.1(2)
C(2)–W(1)–N(3)	98.8(3)	W(1)–C(1)–O(1)	172.2(7)
C(2)–W(1)–N(31)	99.3(3)	W(1)–C(2)–O(2)	174.3(7)
C(2)–W(1)–N(41)	167.5(3)	W(1)–N(3)–C(4)	122.7(4)
C(2)–W(1)–N(51)	91.3(3)	W(1)–N(3)–C(21)	125.6(4)
N(3)–W(1)–N(31)	92.5(2)	C(4)–N(3)–C(21)	111.1(5)

Table 7. Selected Bond Distances (Å) and Angles (deg) for $Tp'(CO)_2W(NMe_2)$ (4c)

W(1)–C(1)	1.952(7)	W(1)–N(31)	2.191(5)
W(1)–C(2)	1.936(6)	C(1)–O(1)	1.156(8)
W(1)–N(3)	1.956(5)	C(2)–O(2)	1.167(8)
W(1)–N(11)	2.238(5)	N(3)–C(4)	1.454(9)
W(1)–N921)	2.239(5)	N(3)–C(5)	1.48(1)
C(1)–W(1)–C(2)	71.8(3)	N(3)–W(1)–N(21)	90.5(2)
C(1)–W(1)–N(3)	93.9(3)	N(3)–W(1)–N(31)	168.6(2)
C(1)–W(1)–N(11)	101.9(3)	N(1)–W(1)–N(21)	85.0(2)
C(1)–W(1)–N(21)	171.8(3)	N(11)–W(1)–N(31)	81.2(2)
C(1)–W(1)–N(31)	95.6(2)	N(21)–W(1)–N(31)	80.9(2)
C(2)–W(1)–N(3)	92.4(3)	W(1)–C(1)–O(1)	173.1(7)
C(2)–W(1)–N(11	173.2(2)	W(1)–C(2)–O(2)	174.3(6)
C(2)–W(1)–N(21)	101.1(2)	W(1)–N(3)–C(4)	128.7(5)
C(2)–W(1)–N(31)	96.6(3)	W(1)–N(3)–C(5)	121.2(4)
N(3)–W(1)–N(11)	90.6(2)	C(4)–N(3)–C(5)	110.1(6)

4a·CH_2Cl_2 [$WC_{30}H_{36}BN_7O_2Cl_2$]: C, 46.30; H, 4.51; N, 12.19. Found: C, 46.74; H, 4.49; N, 12.29.

$Tp'(CO)_2W(N(Me)CH_2Ph)$ (4b). An excess of LDA (4 mmol, 2 mL of a 2 M solution in THF) was added to a blue solution of **1d** (0.55 g, 0.85 mmol) in THF (30 mL) at –40 °C. The resulting solution was a dark red color. Upon addition of excess MeI (1 mL, 8 mmol) the solution color turned blue. After evaporation of the solvent, the greenish residue was chromatographed on an alumina (80–200-mesh) column. A 1:1 mixture of CH_2Cl_2 and hexane eluted a blue band. **4b** was obtained as a blue powder in 50% yield upon evaporation of solvent. ^1H NMR (CD_2Cl_2, δ): 7.5–7.3 (5H, m, Ph), 5.95, 5.80 [3H (1:2), 3 C*H*'s of Tp′], 4.75 (2H, s, CH_2Ph), 2.47, 2.34, 1.73 [18H (9:3:6), 6 CH_3's of Tp′], 2.07 (3H, s, NCH_3). ^{13}C NMR (CD_2Cl_2, δ): 254.7 ($^1J_{WC}$ = 175 Hz, 2 CO), 160.2, 151.3, 146.7, 145.2 [(1:2:1:2), 6 CCH$_3$ of Tp′], 137.8 (ipso C of Ph), 131.2, 128.5 [(2:2), ortho and para C of Ph], 127.8 (para C of Ph), 108.4, 106.6 [(1:2), 3 CH of Tp′], 87.6 (CH_2Ph), 57.2 (NCH_3), 16.6, 15.4, 13.0, 12.6 [(1:2:1:2), 6 CH_3's of Tp′]. Anal. Calcd for **4b**: C, 45.69; H, 4.92; N, 14.91. Found: C, 45.77; H, 4.92; N, 14.85.

$Tp'(CO)_2W(NMe_2)$ (4c). To a solution of complex **1e** (0.40 g, 0.75 mmol) in THF (30 mL) was added 1 equiv of LDA (0.4 mL of a 2 M solution in THF) at –60 °C. The solution turned orange immediately. Addition of MeI (0.1 g, excess) produced a green solution. After removing volatiles under reduced pressure, a blue band was eluted with a 1:1 hexane:dichloromethane mixture from an alumina (80–200-mesh) column. Concentrating the solvent in vacuo and cooling at –30 °C allowed isolation of complex **4c** as blue crystals in 60% yield. ^1H NMR (CD_2Cl_2, δ): 5.94, 5.87 [3H (1:2), 3 C*H*'s of Tp′], 3.30 (3H, s, N*Me*), 2.16 (3H, s, N*Me*′), 2.51, 2.42, 2.36, 1.92 [18H (6:3:3:6), 6 CH_3's of Tp′]. ^{13}C NMR (CD_2Cl_2, δ): 254.8 ($^1J_{WC}$ = 177 Hz, 2 *C*O), 160.0, 151.2, 146.6, 145.6 [(1:2:1:2), 6 *C*CH$_3$ of Tp′], 108.3, 106.6 [(1:2), 3 *C*H of Tp′], 70.6 (N*Me*), 61.4 (N*Me*′), 15.5, 15.0, 13.0, 12.6 [(1:2:1:2), 6 *C*H$_3$'s

Table 8. Atomic Positional Parameters for $[Tp'(CO)_2W(NPh)][PF_6]$ (5b)

atom	*x*	*y*	*z*	B_{iso}, Å^2
W(1)	0.29310(3)	0.02984(4)	0.11561(1)	3.18(2)
C(1)	0.330(1)	–0.1184(9)	0.1649(3)	4.4(5)
O(1)	0.3422(8)	–0.1969(7)	0.1921(3)	6.7(4)
C(2)	0.484(1)	0.0366(1)	0.1007(4)	4.6(5)
O(2)	0.5867(7)	0.0409(8)	0.0916(3)	6.7(4)
N(3)	0.2621(7)	–0.0801(7)	0.0675(3)	3.6(3)
C(4)	0.2573(9)	–0.1674(9)	0.0296(3)	3.6(4)
C(5)	0.148(1)	–0.166(1)	–0.0066(4)	5.2(5)
C(6)	0.145(1)	–0.245(1)	–0.0452(4)	6.2(6)
C(7)	0.248(1)	–0.327(1)	–0.0488(4)	6.7(7)
C(8)	0.353(1)	–0.329(1)	–0.0144(4)	6.3(6)
C(9)	0.359(1)	–0.252(1)	0.0267(4)	5.0(5)
B(1)	0.161(1)	0.293(1)	0.1504(4)	3.5(5)
N(11)	0.1035(7)	0.0580(6)	0.1379(2)	3.2(3)
N(12)	0.0707(6)	0.1766(7)	0.1551(3)	3.1(3)
C(13)	–0.0469(8)	0.1670(9)	0.1708(3)	3.6(4)
C(14)	–0.0904(9)	0.0435(9)	0.1619(4)	4.5(5)
C(15)	0.0042(8)	–0.0222(9)	0.1423(3)	3.6(4)
C(16)	–0.110(1)	0.278(1)	0.1921(4)	5.3(5)
C(17)	0.005(1)	–0.160(1)	0.1258(4)	5.3(5)
N(21)	0.243(7)	0.2068(7)	0.0761(3)	3.8(4)
N(22)	0.1853(7)	0.3060(7)	0.0978(3)	3.8(4)
C(23)	0.165(1)	0.403(1)	0.0656(4)	4.9(5)
C(24)	0.205(1)	0.367(1)	0.0224(4)	5.3(5)
C(25)	0.254(1)	0.243(1)	0.0306(3)	4.5(5)
C(26)	0.107(1)	0.527(1)	0.0793(5)	7.2(7)
C(27)	0.312(1)	0.159(1)	–0.0047(4)	6.0(6)
N(31)	0.3633(7)	0.1564(7)	0.1779(3)	3.6(3)
N(32)	0.2949(7)	0.2692(7)	0.1818(3)	3.5(3)
C(33)	0.3634(9)	0.3442(10)	0.2150(3)	4.4(5)
C(34)	0.4764(9)	0.2804(10)	0.2333(3)	4.6(5)
C(35)	0.4748(8)	0.1634(9)	0.2100(3)	3.9(4)
C(36)	0.3231(12)	0.4785(10)	0.2267(4)	5.7(6)
C(37)	0.5722(9)	0.0556(11)	0.2181(4)	5.7(6)
P(11)	0.6448(7)	0.6271(7)	0.1466(2)	9.1(5)
F(11)	0.7757(10)	0.5468(13)	0.1574(6)	15(2)
F(12)	0.7179(16)	0.7501(10)	0.1701(6)	20(2)
F(13)	0.5138(13)	0.7073(18)	0.1357(6)	30(3)
F(14)	0.5716(15)	0.5041(15)	0.1230(5)	20(2)
F(15)	0.6066(13)	0.5875(14)	0.1977(3)	12(1)
F(16)	0.6830(18)	0.6667(17)	0.0955(4)	22(3)
P(21)	0.64477	0.62709	0.14658	4.3(2)
F(21)	0.79942(3)	0.6256(8)	0.1564(3)	12(1)
F(22)	0.6471(7)	0.77769(12)	0.1388(3)	14(1)
F(23)	0.49012(3)	0.6286(8)	0.1368(3)	9.3(9)
F(24)	0.6424(7)	0.47649(12)	0.1543(3)	8.7(8)
F(25)	0.6392(9)	0.6482(9)	0.20252(7)	13(1)
F(26)	0.6503(9)	0.6060(9)	0.09064(7)	12(1)

Table 9. Selected Bond Distances (Å) and Angles (deg) for $[Tp'(CO)_2W(NPh)][PF_6]$ (5b)

W(1)–C(1)	2.06(1)	W(1)–N(31)	2.218(7)
W(1)–C(2)	2.06(1)	C(1)–O(1)	1.11(1)
W(1)–N(3)	1.755(7)	C(2)–O(2)	1.13(1)
W(1)–N(11)	2.147(7)	N(3)–C(4)	1.39(1)
W(1)–N(21)	2.169(7)		

C(1)–W(1)–C(2)	93.7(4)	N(3)–W(1)–N(11)	103.3(3)
C(1)–W(1)–N(3)	91.1(4)	N(3)–W(1)–N(21)	99.1(3)
C(1)–W(1)–N(11)	90.1(3)	N(3)–W(1)–N(31)	171.2(3)
C(1)–W(1)–N(21)	168.4(3)	N(11)–W(1)–N(21)	82.2(3)
C(1)–W(1)–N(31)	85.0(3)	N(11)–W(1)–N(31)	84.7(3)
C(2)–W(1)–N(3)	87.1(4)	N(21)–W(1)–N(31)	85.7(3)
C(2)–W(1)–N(11)	168.9(3)	W(1)–C(1)–O(1)	175.9(9)
C(2)–W(1)–N(21)	92.3(3)	W(1)–C(2)–O(2)	178.7(9)
C(2)–W(1)–N(31)	85.3(3)	W(1)–N(3)–C(4)	171.6(6)

of Tp′]. Anal. Calcd for **4c**: C, 39.26; H, 4.82; N, 16.87. Found: C, 39.46; H, 4.80; N, 16.82.

Table 10. Atomic Positional Parameters for Tp′(CO)ClW(NTs) (11a)

atom	*x*	*y*	*z*	B_{iso}, Å^2
W(1)	0.72657(6)	0.76523	0.73415(5)	2.58(4)
S(1)	0.9682(6)	0.6703(4)	1.0081(5)	5.0(3)
Cl(1)	0.825(2)	0.7005(8)	0.550(2)	4.4(4)
O(1)	0.814(9)	0.685(4)	0.524(7)	6(2)
Cl(2)	0.511(2)	0.6786(2)	0.745(1)	5.1(5)
O(2)	0.460(3)	0.644(2)	0.752(3)	5.4(7)
N(2)	0.862(2)	0.7201(9)	0.879(1)	3.6(6)
O(3)	1.119(2)	0.710(1)	1.049(2)	6.9(8)
O(4)	0.870(2)	0.656(1)	1.110(1)	6.4(8)
C(11)	1.008(2)	0.579(2)	0.923(2)	5(1)
C(12)	0.947(3)	0.510(2)	0.973(2)	6(1)
C(13)	0.985(3)	0.445(1)	0.912(2)	6(1)
C(14)	1.074(3)	0.4428(1)	0.807(2)	5(1)
C(15)	1.138(3)	0.510(2)	0.768(3)	7(1)
C(16)	1.105(3)	0.580(2)	0.824(3)	7(1)
C(17)	1.109(3)	0.368(2)	0.737(3)	8(1)
B(1)	0.634(2)	0.948(1)	0.671(2)	3(7)
N(21)	0.612(1)	0.8484(8)	0.853(1)	2.8(6)
N(22)	0.597(2)	0.9226(8)	0.811(1)	2.9(5)
C(23)	0.530(2)	0.965(1)	0.905(2)	3.8(7)
C(24)	0.498(2)	0.914(1)	1.009(2)	3.9(8)
C(25)	0.548(2)	0.843(1)	0.972(2)	3.2(7)
C(26)	0.497(3)	1.0487(1)	0.895(2)	5.1(9)
C(27)	0.533(2)	0.767(24)	1.047(1)	3.9(6)
N(31)	0.547(2)	0.820(8)	0.557(1)	2.7(5)
N(32)	0.532(1)	0.8989(8)	0.555(1)	2.8(5)
C(33)	0.421(2)	0.9209(1)	0.439(2)	3.3(7)
C(34)	0.362(2)	0.852(1)	0.366(2)	3.5(8)
C(35)	0.440(2)	0.792(1)	0.442(2)	3.1(8)
C(36)	0.373(3)	1.002(1)	0.403(2)	4.9(9)
C(37)	0.420(3)	0.710(2)	0.407(3)	5(1)
N(41)	0.881(2)	0.8619(8)	0.697(1)	3.2(5)
N(42)	0.822(1)	0.9342(8)	0.671(1)	2.9(5)
C(43)	0.9394(19)	0.983(1)	0.649(2)	3.8(7)
C(44)	1.0857(20)	0.938(1)	0.662(2)	4.3(9)
C(45)	1.0480(18)	0.865(1)	0.695(2)	3.9(8)
C(46)	0.9105(23)	1.066(1)	0.618(2)	4.9(9)
C(47)	1.1566(22)	0.796(1)	0.715(3)	6(1)

Table 11. Selected Bond Distances (Å) and Angles (deg) for Tp′(CO)ClW(NTs) (11a)

W(1)–Cl(1)	2.36(1)	S(1)–N(2)	1.62(1)
W(1)–O(1)	2.65(6)	S(1)–O(3)	1.41(2)
W(1)–Cl(2)	2.33(1)	S(1)–O(4)	1.40(1)
W(1)–N(2)	1.78(1)	S(1)–C(11)	1.83(3)
W(1)–N(21)	2.15(1)	Cl(1)–O(1)	0.36(6)
W(1)–N(31)	2.24(1)	Cl(2)–O(2)	0.74(3)
W(1)–N(41)	2.17(1)		

Cl(1)–W(1)–O(1)	4.8(16)	Cl(2)–W(1)–N(21)	89.6(4)
Cl(1)–W(1)–Cl(2)	95.8(4)	Cl(2)–W(1)–N(31)	84.6(4)
Cl(1)–W(1)–N(2)	96.8(5)	Cl(2)–W(1)–N(31)	166.7(4)
Cl(1)–W(1)–N(21)	163.0(5)	N(2)–W(1)–N(21)	99.0(6)
Cl(1)–W(1)–N(31)	84.6(4)	N(2)–W(1)–N(31)	177.4(6)
Cl(1)–W(1)–N(41)	86.9(5)	N(2)–W(1)–N(41)	99.5(6)
O(1)–W(1)–Cl(2)	91(2)	N(21)–W(1)–N(31)	79.9(5)
O(1)–W(1)–N(2)	98(2)	N(21)–W(1)–N(41)	84.3(5)
O(1)–W(1)–N(21)	163(2)	N(31)–W(1)–N(41)	82.8(4)
O(1)–W(1)–N(31)	83(2)	W(1)–Cl(2)–O(2)	166(3)
O(1)–W(1)–N(41)	91(2)	W(1)–N(2)–S(1)	173(1)
Cl(2)–W(1)–N(2)	93.1(5)		

$[Tp'(CO)_2W(NR)][PF_6]$ (R = Bu^t, 5a; Ph, 5b; Bu^n, 5c; CH_2Ph, 5d). A slight excess of $[Ph_3C][PF_6]$ (0.64g, 1.65 mmol) was added to a solution of the corresponding $Tp'(CO)_2W(NHR)$ complex (**1a–d**) (1.6 mmol) in CH_2Cl_2 (100 mL) at 0 °C. The mixture was stirred at 0 °C for 0.5 h and then allowed to reach room temperature. The solvent was evaporated and the residue was washed with THF (**5a**) or 4 × 50 mL of Et_2O (**5b, 5c, 5d**). Complexes **5a**, **5b**, **5c**, and **5d** were obtained as red, dark purple, purple, and purple-red crystalline materials, respectively, upon crystallization at –20 °C from CH_2Cl_2:Et_2O mixtures. Yields: 85% (**5a**), 86% (**5b**), 78% (**5c**), 83% (**5d**). Data for **5a**: ^1H NMR (CD_2Cl_2, δ) 6.20, 6.10 [3H (2:1), 3 C*H*'s of Tp′], 2.52, 2.47, 2.44, 2.36 [18H (6:3:3:6), 6 C*H*$_3$'s of Tp′], 1.59 [9H, s, C(C*H*$_3$)$_3$]; ^{13}C NMR (CD_2Cl_2, δ) 216.6 ($^1J_{WC}$ = 157 Hz, 2 CO), 154.2, 152.6, 149.8, 148.6 [(1:2:1:2), 6 CCH_3 of Tp′], 109.4, 108.6 [(1:2), 3 CH of Tp′], 74.0 [$^2J_{WC}$ = 23 Hz, *C*(CH$_3$)$_3$], 30.6 [C(*C*H$_3$)$_3$], 17.0, 16.0, 13.2, 12.7 [(2:1:1:2), 6 CH_3's of Tp′]. Anal. Calcd for **5a**·CH_2Cl_2 [$WC_{22}H_{33}BN_7O_2PF_6Cl_2$]: C, 31.53; H, 3.97; N, 11.70. Found: C, 31.88;

H, 4.10; N, 11.52. Data for **5b**: ^{1}H NMR (CD$_2$Cl$_2$, δ) 7.50 (5H, m, N*Ph*), 6.21, 6.06 [3H (2:1), 3 C*H*'s of Tp′], 2.51, 2.46, 2.41, 2.36 [18H (6:3:3:6), 6 C*H*$_3$'s of Tp′]; ^{13}C NMR (CD$_2$Cl$_2$, δ) 216.9 ($^1J_{WC}$ = 153 Hz, 2 *C*O), 153.6 ($^2J_{WC}$ = 31 Hz, ipso C of Ph), 153.7, 153.2, 150.0, 148.3 [(1:2:1:2), 6 *C*CH$_3$ of Tp′], 109.3, 108.6 [(1:2), 3 *C*H of Tp′], 16.2, 15.7, 13.4, 12.7 [(2:1:1:2), 6 *C*H$_3$'s of Tp′], 130.9, 130.2, 127.6 (Ph). Anal. Calcd for **5b**: C, 35.73; H, 3.52; N, 12.68. Found: C, 35.85; H, 3.54; N, 12.30. Data for **5c**: ^{1}H NMR (CD$_2$Cl$_2$, δ) 6.18, 5.98 [3H (2:1), 3 C*H* of Tp′], 3.77 (2H, t, $^3J_{HH}$ = 8 Hz, C*H*$_2$CH$_2$CH$_2$CH$_3$), 2.47, 2.40, 2.36 [18H (12:3:3), 6 C*H*$_3$'s of Tp′], 1.87 (2H, m, CH$_2$C*H*$_2$CH$_2$CH$_3$), 1.44 (2H, m, CH$_2$CH$_2$C*H*$_2$CH$_3$), 0.98 (3H, t, C*H*$_3$ of Bu^n); ^{13}C NMR (CD$_2$Cl$_2$, δ) 216.8 ($^1J_{WC}$ = 158 Hz, 2 *C*O), 153.9, 152.9, 149.8, 148.2 [(1:2:1:2), 6 *C*CH$_3$ of Tp′], 109.2, 108.4 [(1:2), 3 *C*H of Tp′], 67.5 ($^2J_{WC}$ = 26 Hz, *C*H$_2$CH$_2$CH$_2$CH$_3$), 33.4 (CH$_2$*C*H$_2$CH$_2$CH$_3$), 20.5 (CH$_2$CH$_2$*C*H$_2$CH$_3$), 13.4 (*C*H$_3$ of Bu^n), 16.0, 15.9, 13.2, 12.6 [(2:1:1:2), 6 *C*H$_3$ of Tp′]. Anal. Calcd for **5c**: C, 36.29; H, 4.50; N, 14.11. Found: C, 36.24; H, 4.28; N, 13.48. Data for **5d**: ^{1}H NMR (CD$_2$Cl$_2$, δ) 7.5–7.3 (5H, m, Ph), 6.14, 5.93 [3H (2:1), 3 C*H* of Tp′], 4.81 (2H, s, $^2J_{WH}$ = 8 Hz, C*H*$_2$Ph), 2.44, 2.39, 2.31 [18H (6:9:3), 6 C*H*$_3$ of Tp′]; ^{13}C{^{1}H} NMR (CD$_2$Cl$_2$, δ) 216.0 ($^1J_{WC}$ = 155 Hz, 2 *C*O), 154.0, 153.2, 150.0, 148.4 [(1:2:1:2), 6 *C*CH$_3$ of Tp′], 134.6 (ipso C of Ph), 130.0, 129.0 (ortho and meta C of Ph), 129.7 (para C of Ph), 109.3, 108.6 [(1:2), 3 *C*H of Tp′], 71.9 ($^2J_{WC}$ = 27 Hz, *C*H$_2$Ph), 16.0, 13.0, 12.7 [(3:1:2), 6 *C*H$_3$'s of Tp′]. Anal. Calcd for **5d**: C, 36.62; H, 3.71; N, 12.46. Found: C, 35.75; H, 3.85; N, 12.05.

[Tp′(CO)$_2$W(NH)][PF$_6$] (6a) and [Tp′(CO)$_2$W(NCPh$_3$)][PF$_6$] (6b). Tp′(CO)$_2$W(NH$_2$) (**1e**) (1.10 g, 2.0 mmol) was dissolved in CH$_2$Cl$_2$ (20 mL), and the resulting green solution was added dropwise to a cold (−30 °C) [Ph$_3$C][PF$_6$] solution (0.77 g, 2.0 mmol) in CH$_2$Cl$_2$ (20 mL). The reaction mixture turned red. After 15 min of stirring, the solvent was removed under reduced pressure. NMR studies carried out with the reaction mixture revealed the formation of two different complexes in a 4:1 ratio. The two products could be separated by slow crystallization from a 3:1 Et$_2$O:CH$_2$Cl$_2$ mixture. In this way, the complexes [Tp′(CO)$_2$W(NH)][PF$_6$] (**6a**) (major) and [Tp′(CO)$_2$W(NCPh$_3$)][PF$_6$] (**6b**) (minor) were successfully obtained as purple-red and red crystals in yields of 70% and 20%, respectively. Data for **6a**: ^{1}H NMR (CD$_2$Cl$_2$, δ) 9.8 (1H, s, br, N*H*), 6.17, 5.98 [3H (2:1), 3 C*H*'s of Tp′], 2.47, 2.41, 2.37 [18H (12:3:3), 6 C*H*$_3$'s of Tp′]; ^{13}C NMR (CD$_2$Cl$_2$, δ) 215.6 ($^1J_{WC}$ = 159 Hz, 2 *C*O), 153.9, 153.0, 149.9, 148.2 [(1:2:1:2), 6 *C*CH$_3$ of Tp′], 109.4, 108.5 [(1:2), 3 *C*H of Tp′], 16.3, 16.0, 13.3, 12.6 [(2:1:1:2), 6 *C*H$_3$'s of Tp′]. Anal. Calcd for **6a**: 29.28; H, 3.30; N, 14.06. Found: C, 29.81; H, 3.51; N, 13.17. Data for **6b**: ^{1}H NMR (CD$_2$Cl$_2$, δ) 6.05, 5.97 [3H (2:1), 3 C*H*'s of Tp′], 2.50, 2.41, 2.35, 1.73 [18H (6:3:3:6), 6 C*H*$_3$'s of Tp′], 7.4–7.1 (15H, m, 3 Ph); ^{13}C NMR (CD$_2$Cl$_2$, δ) 219.3 ($^1J_{WC}$ = 158 Hz, 2 *C*O), 154.5, 154.0, 150.0, 148.9 [(2:1:1:2), 6 *C*CH$_3$ of Tp′], 142.7 (3 ipso C of 3 Ph), 129.5 (9 ortho and para C of 3 Ph), 129.1 (6 meta C of 3 Ph), 109.6, 109.2 [(1:2), 3 *C*H of Tp′], 93.3 (*C*Ph$_3$), 16.2, 15.3, 13.4, 13.0 [(1:2:1:2), 6 *C*H$_3$'s of Tp′].

Tp′(CO)$_2$W(N═CHR) (R = Pr^n, 7a; R = Ph, 7b). To a solution of [Tp′(CO)$_2$W(NCH$_2$R)][PF$_6$] (R = Pr^n (**5c**) or R = Ph (**5d**)) (1.1 mmol) in CH$_2$Cl$_2$ (40 mL) was added, dropwise, excess Et$_3$N (0.20 mL, 1.4 mmol) until the initial purple-red solution color changed to yellow-green. Volatiles were removed in vacuo. Upon chromatography on an alumina (80–200-mesh) column, a purple (**7a**) or yellow (**7b**) band was eluted using a 1:1 hexane:CH$_2$Cl$_2$ mixture. Following evaporation of solvent, **7a** and **7b** were obtained as a light purple and a lime green powder in 62% and 74% yields, respectively. Data for **7a**: ^{1}H NMR (CD$_2$Cl$_2$, δ) 5.90, 5.89 [3H (2:1), 3 C*H*'s of Tp′], 3.02 (1H, t, $^3J_{HH}$ = 6 Hz, $^3J_{WH}$ = 6 Hz, C*H*Pr^n), 2.77 (2H, m, C*H*$_2$CH$_2$CH$_3$), 2.46, 2.43, 2.36, 2.27 [18H (6:3:3:6), 6 C*H*$_3$'s of Tp′], 1.40 (2H, m, CH$_2$C*H*$_2$CH$_3$), 0.93 (3H, t, $^3J_{HH}$ = 7 Hz, C*H*$_3$); ^{13}C NMR (CD$_2$Cl$_2$, δ) 241.7 ($^1J_{WC}$ = 174 Hz, 2 *C*O), 157.5, 152.1, 146.5, 145.4 [(1:2:1:2), 6 *C*CH$_3$ of Tp′], 150.0 ($^2J_{WC}$ = 27 Hz, *C*HPr^n), 107.8, 106.7 [(1:2), 3 *C*H of Tp′], 16.4, 16.3, 12.9, 12.7 [(2:1:1:2), 6 *C*H$_3$'s of Tp′], 28.0 (*C*H$_2$CH$_2$CH$_3$), 23.2 (CH$_2$*C*H$_2$CH$_3$), 13.9 (*C*H$_3$ of Pr^n). Anal. Calcd for **7a**: C, 41.54; H, 4.98. Found: C, 41.06; H, 5.23. Data for **7b**: ^{1}H NMR (CD$_2$Cl$_2$, δ) 7.4–7.0 (5H, m, Ph), 5.91, 5.87 [3H (1:2), 3 C*H*'s of Tp′], 3.79 (1H, $^3J_{WH}$ = 4 Hz, C*H*Ph), 2.44, 2.36, 2.23 [18H (9:3:6), 6 C*H*$_3$'s of Tp′]; ^{13}C NMR (CD$_2$Cl$_2$, δ) 239.1 ($^1J_{WC}$ = 171 Hz, 2 *C*O), 156.7, 152.2, 146.7, 145.6 [(1:2:1:2), 6 *C*CH$_3$ of Tp′], 147.3 ($^2J_{WC}$ = 26 Hz, *C*HPh), 128.4 (para C of Ph), 128.2 (ipso C of Ph), 128.1, 126.9 (ortho and meta C of Ph), 107.9, 106.8 [(1:2), 3 *C*H of Tp′], 16.5, 16.3, 12.9, 12.7 [(2:1:1:2), 6 *C*H$_3$'s of Tp′]. Anal. Calcd for **7b**: C, 44.96; H, 4.40; N, 15.29. Found: C, 45.36; H, 4.54; N, 14.85.

Tp′(CO)(CHO)W(NPh) (8). A CD$_3$CN solution (0.06 mL) of lithium borohydride (8.4 mg, 0.38 mmol) and a CD$_2$Cl$_2$ solution (0.20 mL) of complex **5b** (30 mg, 0.038 mmol) were frozen together and sealed under vacuum in an NMR tube before mixing. After thawing and mixing, the solution color changed from purple to green, which indicated that complex **8** had formed. ^{1}H NMR (CD$_3$CN/CD$_2$Cl$_2$, δ) at −70 °C: 16.30 (1H, s, br, C*H*O), 7.30 (5H, s, C$_6$*H*$_5$), 6.01, 5.94, 5.83 [3H (1:1:1), 3 C*H*'s of Tp′], 2.41, 2.34, 2.28, 2.19, 2.04 [18H (3:3:3:3:6), 6 C*H*$_3$'s of Tp′]. ^{13}C NMR (CD$_3$CN/CD$_2$Cl$_2$, δ): 156.1, 129.7, 127.1, 125.6 (*C*$_6$H$_5$), 152.8, 152.1, 146.9, 146.8, 146.6 [(1:2:1:1), 6 *C*CH$_3$ of Tp′], 107.8, 107.7, 107.1 [(1:1:1), 3 *C*H of Tp′], 15.5, 15.4, 14.9, 13.1, 13.1, 12.6, 12.3 [(1:1:1:1:1:1), 6 *C*H$_3$'s of Tp′].

Tp′(*CO)(*CHO)W(NPh). (a) Tp′(*CO)$_3$WI. A dark red THF solution of Tp′(CO)$_3$WI (2 g, 2.9 mmol) was heated for 4 h at reflux. Tp′(CO)$_2$WI [IR (CH$_2$Cl$_2$): 1945, 1850 cm^{-1}] was isolated as a yellow powder after solvent evaporation. The yellow solid was dissolved in THF (80 mL) and sealed in a 150-mL flask under ^{13}C labeled *CO (70 mL, 3.1 mmol). The solution color changed from yellow to dark red in 4 h. The infrared spectrum showed four carbonyl absorptions at 2015, 2000, 1917 (broad), and 1886 (broad) cm^{-1}, indicating that the ^{13}C labeled Tp′(*CO)$_3$I (ca. 33% enrichment) was formed.

(b) Tp′(*CO)$_2$W(NHPh). This complex was synthesized from Tp′(*CO)$_3$WI by following the procedure described under method A for the preparation of complex **1b**.

(c) [Tp′(*CO)$_2$W(NPh)][PF$_6$]. This complex was synthesized from Tp′(*CO)$_2$W(NHPh) by the procedure described for complex **5b**. The infrared spectrum in methylene chloride shows two absorptions at 2060 and 1976 cm^{-1}, corresponding to the ^{13}C labeled complex, plus two absorptions at 2079 and 2004 cm^{-1}, corresponding to the unlabeled complex.

(d) Tp′(*CO)(*CHO)W(NPh). The ^{13}C labeled complex **8** was synthesized as described above for **8** using the ^{13}C labeled complex [Tp′(*CO)$_2$W(NPh)][PF$_6$]. ^{13}C NMR (CD$_3$CN, δ): 293 ($^1J_{HC}$ = 133 Hz, CHO), 259 (*C*O).

Tp′(CO)$_2$W(N) (9). Method A. Complex **6a** (0.3 g, 0.43 mmol) was dissolved in THF and stirred with excess KH (1 g) for 5 min. The reaction mixture was centrifuged to give an orange-red solution of complex **9** suitable for reactions. Attempts to isolate this new species failed due to decomposition during workup. Spectroscopic data and chemical behavior are in accord with the Tp′(CO)$_2$W(N) formulation for complex **9**. **Method B.** A solution of **2** (0.50 g, 0.75 mmol) in CH$_2$Cl$_2$ (20 mL) was added slowly to a CH$_2$Cl$_2$ solution (15 mL) of [(Ph$_3$P)$_2$N][N$_3$] (0.44 g, 0.75 mmol) with stirring at −78 °C. The resulting red-orange solution was stirred at −78 °C for 15 min before Et$_2$O (150 mL) was added to precipitate a white crystalline solid ((Ph$_3$P)$_2$NI). After filtering, this solution was suitable for further reactions. Data for **9**: ^{1}H NMR (THF-*d*$_8$, δ): 6.05, 5.74 [3H (2:1), 3 C*H*'s of Tp′], 2.70, 2.40, 2.30, 2.22 [18H (6:3:3:6), 6 C*H*$_3$'s of Tp′].

[Tp′(CO)$_2$W(NMe)][PF$_6$] (10). MeOTf (30 μL, 1 equiv) was added to a cold solution (−60 °C) of complex **9** (0.3 mmol) in THF (20 mL). The mixture was stirred for 5 min and then evaporated to dryness. The residue was extracted with CH$_2$Cl$_2$, and excess [NH$_4$][PF$_6$] (0.2 g) was added. After stirring for 6 h, the resulting solution was centrifuged, the solvent was removed in vacuo, and the residue was extracted with CH$_2$Cl$_2$ (4 mL). Hexane (15 mL) was added as a second layer for slow diffusion. Red crystals of [Tp′(CO)$_2$W(NMe)][PF$_6$] (**10**) appeared at room temperature after several hours. Yield: 70%. Data for **10**: ^{1}H NMR (CD$_2$Cl$_2$, δ) 6.15, 5.95 [3H (2:1), 3 C*H*'s of Tp′], 3.67 (3H, $^3J_{WH}$ = 10 Hz, NC*H*$_3$), 2.45, 2.38, 2.35 [18H (12:3:3), 6 C*H*$_3$'s of Tp′]; ^{13}C

NMR (CD_2Cl_2, δ) 216.6 (2 CO), 154.0, 153.2, 149.9, 148.3 [(1:2:1:2), 6 CCH$_3$ of Tp′], 109.3, 108.6 [(1:2), 3 *C*H of Tp′], 55.9 (N*C*H$_3$), 16.0, 15.9, 13.3, 12.7 [(1:2:1:2), 6 *C*H$_3$'s of Tp′]. Anal. Calcd for **10**: C, 30.39; H, 3.51; N, 13.79. Found: C, 31.26; H, 3.52; N, 13.66.

Tp′(CO)ClW(NTs) (11a). To a stirred solution of **9** (0.75 mmol) in CH_2Cl_2/Et_2O at −78 °C was added TsCl (0.14 g, 0.75 mmol) (Ts = $-SO_2C_6H_4CH_3$) in CH_2Cl_2 (5 mL). After evaporation of solvent, the reddish oily residue was washed with MeOH (2 × 20 mL). The complex was obtained as a blue solid by crystallization at room temperature from a mixture of CH_2Cl_2 (10 mL) and Et_2O (40 mL). After further washing (2 × 20 mL of Et_2O) and slow diffusion in CH_2Cl_2/Et_2O, single crystals suitable for X-ray were obtained. Yield: 48%. Data for **11a**: ^{1}H NMR (CD_2Cl_2, δ) 7.77, 7.36 (4H, $J_{\mathrm{app\,HH}}$ = 8 Hz, AA′XX′, $C_6H_4CH_3$), 6.11, 6.07, 5.69 [3H (1:1:1), 3 C*H*'s of Tp′], 2.59, 2.53, 2.50, 2.44, 2.34, 2.24 [21H (3:3:3:3:6:3), 6 C*H*$_3$'s of Tp′ and *p*-C*H*$_3$ of Ts]; ^{13}C NMR (CD_2Cl_2, δ) 279.8 (*C*O), 155.8, 153.8, 153.6, 147.7, 147.2, 146.1, 145.4 [(1:1:1:1:1:1:1), 6 *C*CH$_3$ of Tp′ and ipso or para C of Ts], 135.3 [ipso or para C of Ts], 130.0 [ortho or meta C of Ts], 128.5 [ortho of meta C of Ts], 109.0, 108.1, 107.8 [(1:1:1), 3 *C*H of Tp′], 21.8 [*p*-*C*H$_3$ of Ts], 17.4, 15.5, 15.0, 12.9, 12.6, 12.5 [(1:1:1:1:1:1), 6 *C*H$_3$'s of Tp′]. Anal. Calcd for **11a**: C, 38.70; H, 4.10; N, 13.74; Cl, 4.97. Found: C, 38.65; H, 4.08; N, 13.80; Cl, 5.09.

Tp′(CO)ClW(NC(O)CH$_3$) (11b). To a stirred solution of **9** (0.8 mmol) in CH_2Cl_2/Et_2O at −78 °C was added 0.62 mL of a 1.3 M solution of acetyl chloride in CH_2Cl_2. Volatiles were removed in vacuo, and Et_2O (10 mL) was added. The resulting solution was centrifuged. The solvent was evaporated, and MeOH (7 mL) was added to extract the blue product. After partial evaporation of the solvent and cooling to −30 °C, analytically pure, blue crystalline material was isolated. Yield: 33%. Data for **11b**: ^{1}H NMR (C_6D_6, δ) 5.57, 5.42, 5.11 [3H (1:1:1), 3 C*H*'s of Tp′], 2.91, 2.57, 2.23, 2.06, 2.02, 1.79 [18H (3:3:3:3:3:3), 6 C*H*$_3$'s of Tp′], 1.73 [3H, C(O)C*H*$_3$]; ^{13}C NMR (C_6D_6, δ) 280.6 ($^1J_{\mathrm{WC}}$ = 177 Hz, *C*O), 180.9 [$^2J_{\mathrm{WC}}$ = 35 Hz, N*C*(O)CH$_3$], 153.4, 153.3, 153.2, 146.0, 145.2, 144.5 [(1:1:1:1:1:1), 6 *C*CH$_3$ of Tp′], 108.5, 108.0, 107.8 [(1:1:1), 3 *C*H of Tp′], 31.9 (C(O)*C*H$_3$], 16.9, 15.6, 12.5, 12.4, 12.3 [(1:2:1:1:1:1), 6 *C*H$_3$'s of Tp′]. Anal. Calcd for **11b**: C, 35.94; H, 4.19; N, 16.30; Cl, 5.89. Found: C, 36.02; H, 4.29; N, 16.11; Cl, 5.73.

Tp′(CO)(OC(O)CH$_3$)W(NC(O)CH$_3$) (11c). To a stirred solution of **9** (0.75 mmol) in CH_2Cl_2/Et_2O at −78 °C was added 1 equiv of acetic anhydride (86 μL). After 10 min, the reaction mixture was evaporated to dryness. The reddish oil was dissolved in 15 mL of a 1:2 mixture of CH_2Cl_2/MeOH. This solution was cooled to −30 °C. After 2 days, a green filtrate was removed. The volume of this filtrate was reduced until a reddish brown precipitate was observed. The blue filtrate was removed, and partial evaporation of the solvent led to isolation of the complex as a light blue powder in 36% yield. Attempts to obtain elemental analyses of this complex were unsuccessful due to decomposition in the solid state. Data for **11c**: ^{1}H NMR (C_6D_6, δ) 5.62, 5.59, 5.26 [3H (1:1:1), 3 C*H*'s of Tp′], 2.68, 2.39, 2.35, 2.31, 2.25, 2.22, 2.15, 1.95 [24H (3:3:3:3:3:3:3:3), 6 C*H*$_3$'s of Tp′, OC(O)C*H*$_3$, and NC(O)C*H*$_3$]; ^{13}C NMR (CD_2Cl_2, δ) 284.8 ($^1J_{\mathrm{WC}}$ = 185, *C*O), 181.7 [$^2J_{\mathrm{WC}}$ = 35 Hz, N*C*(O)CH$_3$], 175.7 [O*C*(O)CH$_3$], 152.9, 152.3, 146.3, 145.2, 145.0 [(1:2:1:1:1:1), 6 *C*CH$_3$ of Tp′], 108.0, 107.9, 107.4 [(1:1:1), 3 *C*H of Tp′], 24.4, 23.2 [NC(O)*C*H$_3$ and OC(O)*C*H$_3$], 16.7, 14.7, 14.4, 12.3, 12.0 [(1:1:1:2:1), 6 *C*H$_3$ of Tp′].

X-ray Crystallographic Analyses of Tp′(CO)$_2$W(N(Ph)CH$_2$Ph)·CH$_2$Cl$_2$ (4a·CH$_2$Cl$_2$), Tp′(CO)$_2$W(NMe$_2$) (4c), [Tp′(CO)$_2$W(NPh)][PF$_6$] (5b), and [Tp′(CO)(Cl)W(NTs)] (11a). Green crystals of **4a**·CH_2Cl_2 were grown by slow diffusion of a CH_2Cl_2 solution of **4a** into hexane. Blue crystals of **4c** were grown by slow diffusion of a CH_2Cl_2 solution of **4c** into hexane. Purple crystals of **5b** and large blue crystals of **11a** were grown by slow diffusion of a CH_2Cl_2 solution of the respective complex into Et_2O. In each case, an appropriate crystal was selected (**4a**, **4c**, and **5b**) or cut (**11a**), mounted on a glass wand, and then coated with epoxy. Diffraction data were collected on an Rigaku AFC6/S diffractometer (**4a**, **4c**, and **11a**) or an Enraf-Nonius CAD-4 diffractometer (**5b**). Crystal data collection parameters are summarized in Table 3. Cell dimensions were obtained for **4a**·CH_2Cl_2 from 41 centered reflections in the region 35.0° < 2θ < 40.0°, for **4c** from 25 centered reflections in the region 22.4° < 2θ < 28.1°, for **5b** from 25 centered reflections in the region 30.0° < 2θ < 35.0°, and for **11a** from 46 centered reflections in the region 30.0° < 2θ < 40.0° and refined by least squares calculations. Intensity diffraction data were collected in the quadrant $\pm h,+k,\pm l$ for **4a** and **4c** and $\pm h,+k,+l$ for **5b** and **11a**. Only data with $I > 2.5\sigma(I)$ were used in structure solution and refinement.[42] The data were corrected for Lorentz and polarization effects during the final stages of data reduction. The minimum and maximum transmission factors were 0.494 and 0.500 (**4a**), 0.316 and 0.435 (**4c**), and 0.396 and 0.489 (**5b**). Absorption corrections were made using ψ scans for **4c**, and no absorption correction was made for **11a**. The crystal was checked for orientation every 100 (**4a**, **4c**, and **11a**) or every 200 reflections (**5b**) and was recentered if necessary. The position of the tungsten was deduced by direct methods (**4a**, **4c**, **11a**) or from the three-dimensional Patterson function (**5b**). The positions of the remaining non-hydrogen atoms were determined through subsequent difference Fourier syntheses and were refined anisotropically. Hydrogen atom positions were calculated by using a C–H distance of 0.96 Å and an isotropic thermal parameter calculated from the anisotropic values for the atoms to which they were connected. The structure for **11a** appeared to have disorder of the Cl and CO ligands attached to the tungsten which was modeled as 60% Cl/40% CO [Cl(1), O(1)] and 40% Cl/60% CO [Cl(2), O2], and the Cl atoms were given composite scattering factors. The final residuals[43,44] for **4a**·CH_2Cl_2 for 397 variables refined against 3910 data with $I > 2.5\sigma(I)$ were R = 0.037 and R_w = 0.046.[45] The final residuals for **4c** for 272 variables refined against 4208 data with $I > 2.5\sigma(I)$ were R = 0.039 and R_w = 0.043. The final residuals for **5b** for 401 variables refined against 2885 data with $I > 2.5\sigma(I)$ were R = 0.036 and R_w = 0.045. The final residuals for **11a** for 332 variables refined against 2017 data with $I > 2.5\sigma(I)$ were R = 0.040 and R_w = 0.046. The final difference Fourier maps for **4a**·CH_2Cl_2, **4c**, **5b**, and **11a** had no peak greater than 1.990, 1.700, 0.68, and 3.150 e/Å^3, respectively.

Acknowledgment. We are grateful to the National Institutes of Health (Grant GM28938) and the Department of Energy (Grant DE-FG05-85ER13430) for financial support. P.J.P. also thanks the Ministerio de Educacion y Ciencia (Spain) for a research studentship.

Supplementary Material Available: Tables SI–SXVI with complete bond distances and angles, atomic coordinates, and thermal parameters for complexes **4a**, **4c**, **5b**, and **11a** (21 pages). Ordering information is given on any current masthead page.

OM9308811

---

(42) Programs used during solution and refinement were made from the NRCVAX structure determination package. Gabe, E. J.; Le Page, Y.; Charland, J. P.; Lee, F. L.; White, P. S. *J. Appl. Chem.* **1989**, *22*, 384.

(43) The function minimized was $\sum w(|F_o| - |F_c|)^2$, where w is based on counting statistics.

(44) Scattering factors were taken from the following: Cromer, D. T.; Waber, J. T. In *International Tables for X-Ray Crystallography*; Ibers, J. A., Hamilton, J. C., Eds.; Kynoch Press: Birmingham, England, 1974; Vol. IV, Table 2.2.

(45) $R_{\mathrm{unweighted}} = \sum(|F_o| - |F_c|)/\sum|F_o|$ and $R^*_{\mathrm{weighted}} = [\sum w(|F_o| - |F_c|)^2/\sum wF_o^2]^{1/2}$.